

1 **Viral mimicry of p65/RelA transactivation domain to inhibit NF- $\kappa$ B activation**

2

3 Jonas D. Albarnaz<sup>1\*</sup>, Hongwei Ren<sup>1†</sup>, Alice A. Torres<sup>1</sup>, Evgeniya V. Shmeleva<sup>1‡</sup>, Carlos A.  
4 Melo<sup>2</sup>, Andrew J. Bannister<sup>2</sup>, Geoffrey L. Smith<sup>1\*</sup>

5 <sup>1</sup>Department of Pathology, University of Cambridge, Cambridge CB2 1QP, UK

6 <sup>2</sup>The Gurdon Institute, University of Cambridge, Cambridge CB2 1QN, UK

7

8 \*Corresponding authors: [gl37@cam.ac.uk](mailto:gl37@cam.ac.uk) (GLS); [jd732@cam.ac.uk](mailto:jd732@cam.ac.uk) (JDA)

9

10 †Present address: Department of Immunology and Inflammation, Imperial College  
11 London, Hammersmith Campus, Du Cane Road, London W12 0NN, UK

12 ‡Present address: Department of Obstetrics and Gynaecology, University of Cambridge, Box  
13 223, Level 2, The Rosie Hospital, Robinson Way, Cambridge CB2 2SW, UK

14

15 Running title: Viral inhibition of NF- $\kappa$ B via molecular mimicry

16

17 Key words: vaccinia virus, NF- $\kappa$ B, molecular mimicry, p65, CBP, BRD4, virulence, immune  
18 evasion, poxvirus

1 ABSTRACT

2 The evolutionary arms race between hosts and their viruses drove the evolution of complex  
3 immune systems in mammals and sophisticated immune evasion mechanisms by viruses.  
4 Mammalian antiviral defences require sensing of virus infection and stimulation of the  
5 expression of interferons and cytokines via the activation of NF- $\kappa$ B and other immune  
6 signalling pathways. Viruses antagonise these host antiviral defences by interfering with  
7 immune sensing and signal transduction and blocking the actions of interferons and  
8 cytokines. Here we show that a viral protein mimics the transcription activation domain of  
9 p65, the transcriptionally active subunit of NF- $\kappa$ B. The C terminus of vaccinia virus (VACV)  
10 protein F14 (residues 51-73) activates transcription when fused to a DNA-binding domain-  
11 containing protein and associates with NF- $\kappa$ B co-activator CBP, disrupting its interaction with  
12 p65. Consequently, F14 diminishes CBP-mediated acetylation of p65 and the downstream  
13 recruitment of RNA polymerase II processivity factor BRD4 to the promoter of NF- $\kappa$ B-  
14 responsive gene *CXCL10*, thereby inhibiting the expression and secretion of CXCL10 upon  
15 stimulation with TNF- $\alpha$ . A VACV strain engineered to lack F14 caused reduced lesions in an  
16 intradermal model of infection, showing that F14 contributes to virulence. Our results  
17 uncover a mechanism by which viruses disarm the antiviral defences through molecular  
18 mimicry of a conserved protein of the host's immune system.

19

## 1 INTRODUCTION

2 Viruses provide constant selective pressure shaping the evolution of the immune systems of  
3 multicellular organisms [1-3]. At the cellular level, an array of receptors detect virus-derived  
4 molecules, or more broadly pathogen-associated molecular patterns (PAMPs), allowing the  
5 recognition of invading viruses and the activation of a gene expression programme that  
6 initiates the antiviral response [reviewed by [4, 5]]. The induced gene products, which  
7 include interferons, cytokines and chemokines, are secreted and function as signals to  
8 activate more specialised immune cells and attract them to the site of infection, thereby  
9 generating inflammation [reviewed by [6-8]]. This coordinated inflammatory response  
10 evolved to achieve the control and (or) elimination of the infection, and the establishment of  
11 an immunological memory against future infection [reviewed by [4, 9]].

12 Engagement of pattern recognition receptors (PRRs) by their cognate PAMPs activates  
13 multiple transcription factors, including nuclear factor kappa light-chain enhancer of activated  
14 B cells (NF- $\kappa$ B) [reviewed by [10-12]]. NF- $\kappa$ B is a homo- or heterodimer of Rel proteins, with  
15 the heterodimer of p50 (also known as NF- $\kappa$ B1 or NFKB1) and p65 (also known as RelA or  
16 RELA) being the prototypical form of NF- $\kappa$ B [13]. Through an interface formed by the Rel  
17 homology domains of the two Rel subunits, NF- $\kappa$ B recognises and binds to a consensus  
18 DNA sequence in the promoter elements and enhancers of target genes [reviewed by [10],  
19 [14]]. NF- $\kappa$ B-responsive gene products include inflammatory mediators, such as cytokines,  
20 chemokines and cell adhesion molecules, as well as proteins involved in other immune  
21 processes, like MHC molecules, growth factors and regulators of apoptosis [15, 16].  
22 Moreover, cytokines, such as interleukin (IL)-1 and tumour necrosis factor (TNF)- $\alpha$ , also  
23 trigger NF- $\kappa$ B activation upon engagement of their receptors on the cell surface [reviewed by  
24 [10, 11]].

25 In resting conditions, NF- $\kappa$ B remains latent in the cytoplasm bound to the inhibitor of  $\kappa$ B  
26 ( $\text{I}\kappa\text{B}$ )  $\alpha$  (also known as NFKBIA) [17, 18]. Upon activation, the  $\text{I}\kappa\text{B}$  kinase (IKK) complex  
27 phosphorylates  $\text{I}\kappa\text{B}\alpha$ , triggering its ubiquitylation and subsequent proteasomal degradation,  
28 thus releasing NF- $\kappa$ B to accumulate in the nucleus [18] [reviewed by [10, 11]]. In the  
29 nucleus, NF- $\kappa$ B interacts with chromatin remodelling factors, coactivators and general  
30 transcription factors to activate the transcription of antiviral and inflammatory genes by RNA  
31 polymerase (RNAP) II [14, 19-24]. The specificity and kinetics of NF- $\kappa$ B-dependent gene  
32 expression is determined by several factors including dimer composition [25], cooperation  
33 with other transcription factors [the cooperation between NF- $\kappa$ B, activator protein (AP)-1 and  
34 interferon regulatory factor (IRF) transcription factors to activate interferon (IFN)- $\beta$   
35 transcription in response to virus infection being a classical example [26]], duration of the  
36 stimulus [27, 28], cell type [29, 30] and chromatin context on the promoters of target genes  
37 [14, 31, 32]. In addition, NF- $\kappa$ B undergoes multiple posttranslational modifications, in the  
38 cytoplasm or nucleus, that control its transcriptional activity through interactions with  
39 coactivators and basal transcription machinery [reviewed by [13, 33, 34]].

40 Following the stimulation with PAMPs (e.g. lipopolysaccharide) or inflammatory cytokines  
41 (e.g. TNF- $\alpha$ ), two conserved residues in p65 are phosphorylated: Ser<sup>276</sup>, mainly by protein  
42 kinase A (PKA), and Ser<sup>536</sup> within the transactivation domain (TAD), by the IKK complex [35,  
43 36]. Phosphorylation of either site enhances NF- $\kappa$ B transcriptional activity by promoting the  
44 interaction with the coactivators CREB-binding protein (CBP) or its paralogue p300 (also  
45 known as CREBBP and EP300, respectively). These coactivators acetylate p65 at Lys<sup>310</sup> as  
46 well as histones on the target gene promoters to allow transcription initiation and elongation  
47 to proceed [36-39]. The bromodomain and extraterminal domain (BET) protein BRD4 docks

1 onto acetylated p65 Lys<sup>310</sup> via its two bromodomains and subsequently recruits positive  
2 transcription elongation factor b (P-TEFb) to drive transcription of inflammatory genes by  
3 RNAP II [40]. This latter study highlighted the complexity of the gene expression programme  
4 downstream of NF- $\kappa$ B, with subsets of genes differentially expressed depending on the  
5 transcriptional regulatory events following NF- $\kappa$ B recruitment to DNA [[40-42]; reviewed by  
6 [43]].

7 The confrontations between viruses and hosts leave genetic signatures over their  
8 evolutionary histories [3, 44]. On one hand, host innate immune factors display strong signs  
9 of positive selection to adapt to the pressure posed by viruses [reviewed by [45]]. On the  
10 other hand, viruses acquire multiple mechanisms to antagonise host innate immunity, such  
11 as mimicking host factors to disrupt their functions in the antiviral response or to subvert  
12 them for immune evasion [reviewed by [45, 46]]. Poxviruses have been a paradigm in the  
13 study of virus-host interactions [reviewed by [47]]. Their large DNA genomes encode a  
14 plethora of proteins that antagonise the host antiviral response. Some poxvirus proteins  
15 show structural similarity to host proteins and modulate innate immune signalling during  
16 infection [reviewed by [48, 49]].

17 Vaccinia virus (VACV), the smallpox vaccine and the prototypical poxvirus, utilises molecular  
18 mimicry to antagonise the host response to infection [reviewed by [50]]. VACV-encoded  
19 soluble receptors of TNF and IL-1 $\beta$  share amino acid similarity with their cellular  
20 counterparts and bind to extracellular cytokines to block the engagement of the cognate  
21 cellular receptors and thereby the activation of downstream signalling pathways, including  
22 NF- $\kappa$ B [reviewed by [50, 51]]. VACV also encodes a family of proteins sharing structural  
23 similarity to cellular Bcl-2 proteins despite very limited sequence similarity. Viral Bcl-2-like  
24 proteins have evolved to perform a wide range of functions, such as inhibition of NF- $\kappa$ B  
25 activation [reviewed by [52]]. One example is VACV protein A49, which notwithstanding its  
26 Bcl-2 fold, also mimics the I $\kappa$ B $\alpha$  phosphodegron that is recognised by the E3 ubiquitin ligase  
27  $\beta$ -TrCP, thereby blocking I $\kappa$ B $\alpha$  ubiquitylation [53, 54]. Upon NF- $\kappa$ B activation, the IKK  
28 complex phosphorylates A49 to create the complete phosphodegron mimic that then  
29 engages with  $\beta$ -TrCP to prevent I $\kappa$ B $\alpha$  ubiquitylation [55].

30 Previous work from our laboratory predicted that VACV encodes additional inhibitors of NF-  
31  $\kappa$ B because a mutant VACV strain (vv811 $\Delta$ A49) lacking the function of all known inhibitors of  
32 NF- $\kappa$ B still suppresses NF- $\kappa$ B-dependent gene expression without preventing NF- $\kappa$ B  
33 translocation to the nucleus [56]. Here, we mapped this NF- $\kappa$ B inhibitory activity to the open  
34 reading frame (ORF) *F14L*, which is conserved across all orthopoxviruses including the  
35 human pathogens variola, monkeypox and cowpox viruses. Using a combination of gene  
36 expression and protein-based assays, we show that F14 from VACV inhibits NF- $\kappa$ B when  
37 expressed ectopically or during infection. Furthermore, a VACV strain lacking F14 has  
38 reduced virulence in a mouse model. Mechanistically, the F14 C terminus mimics the  
39 transactivation domain (TAD) of p65 and outcompetes p65 for binding to the coactivator  
40 CBP. As a consequence, F14 reduces p65 acetylation and downstream molecular events  
41 required for the activation of a subset of NF- $\kappa$ B-responsive inflammatory genes.

42

## 1 RESULTS

### 2 *Vaccinia virus protein F14 is a virulence factor that inhibits NF- $\kappa$ B activation*

3 The prediction that VACV encodes additional inhibitor(s) of NF- $\kappa$ B that function downstream  
4 of p65 translocation into the nucleus [56], prompted a search for nuclear NF- $\kappa$ B inhibitors.  
5 VACV strain vv811 $\Delta$ A49 lacks 56 ORFs, but retains the inhibitor(s) [56, 57], and so its  
6 encoded proteins were screened by bioinformatics for ones that met the following criteria: (i)  
7 early expression, based on previous VACV transcriptome studies [58, 59]; (ii) predicted not  
8 to be involved in replication and/or morphogenesis; (iii) being poorly characterised; (iv)  
9 presence of putative nuclear localisation signals (NLS) or predicted molecular mass <40 kDa  
10 that would allow diffusion into the nucleus [60]; and (v) the presence of domains indicative of  
11 function. The genomic position of the ORF and its conservation among orthopoxviruses were  
12 also considered given that VACV immunomodulatory genes are located towards the genome  
13 termini and are sometimes less conserved than genes centrally located that have functions  
14 in virus replication [61].

15 This approach yielded a list of seven ORFs, namely *F6L*, *F7L*, *F14L*, *A47L*, *B6R*, *B11R* and  
16 *B12R*. These ORFs were codon-optimised for expression in human cells, cloned into  
17 pcDNA4/TO and tested for inhibition of NF- $\kappa$ B activation in an NF- $\kappa$ B luciferase reporter  
18 gene assay. Protein F14 inhibited TNF- $\alpha$  and IL-1 $\beta$ -stimulated NF- $\kappa$ B activity in HEK 293T  
19 cells in a dose-dependent manner (Figure 1A, B and Figure S1). This inhibitory activity was  
20 specific for the NF- $\kappa$ B pathway, because F14 did not affect IFN- $\alpha$ -stimulated Janus kinase  
21 (JAK)/signal transducer and activators of transcription (STAT) or phorbol 12-myristate 13-  
22 acetate (PMA)-stimulated mitogen-activated protein kinase (MAPK)/AP-1 pathways (Figure  
23 1C, D). The inhibitory activity was exerted despite the lower levels of F14 expression when  
24 compared to VACV protein B14, a known inhibitor of NF- $\kappa$ B (Figure 1E) [62]. Conversely,  
25 VACV protein C6 suppressed type I IFN signalling and B14 upregulated AP-1 activity, as  
26 observed previously (Figure 1C, D) [63, 64].

27 Most VACV immunomodulatory proteins affect virulence in intranasal or intradermal murine  
28 models [reviewed by [50, 51]]. To evaluate if loss of F14 expression affected virulence, a  
29 recombinant VACV lacking F14 was generated, termed  $\Delta$ F14. Intradermal inoculation of the  
30 ear pinnae of mice with  $\Delta$ F14 produced smaller lesions, and reduced virus titres at 7 and 10  
31 d post-infection (p.i.) (Figure 1F, G) compared to wild type virus (vF14) and a revertant strain  
32 (vF14-Rev), generated by reinserting F14 into  $\Delta$ F14 at its natural locus (Figure 1F).  
33 Attenuation of  $\Delta$ F14 in the intradermal mouse model correlated with reduced viral titres in  
34 the infected ears 7 and 10 d p.i., but not 3 d p.i. (Figure 1G). In contrast, in an intranasal  
35 mouse model  $\Delta$ F14 caused the same extent of body mass loss as wild type and revertant  
36 controls (Figure S2). In cell culture, vF14,  $\Delta$ F14 and vF14-Rev displayed no differences in  
37 replication and plaque size (Figure S3). Altogether, these experiments showed that F14 is  
38 not essential for virus replication but makes a modest contribution to virulence.

39 Previous analyses of VACV transcriptome showed that the *F14L* ORF is transcribed and  
40 translated early during infection [58, 59, 65]. This was consistent with an upstream typical  
41 early promoter and a transcription termination motif T<sub>5</sub>NT downstream of the stop codon [66,  
42 67]. To investigate F14 expression during infection, a VACV strain was constructed in which  
43 F14 was tagged with a C-terminal TAP tag. The vF14-TAP strain replicated normally (Figure  
44 S3) and immunoblotting showed F14 expression from 4 h p.i. and peaked by 8 h p.i.,  
45 matching the accumulation of another early VACV protein C6 (Figure 1H) [68]. F14 levels  
46 were notably lower compared to other VACV proteins tested either when expressed  
47 ectopically (Figure 1E) or during infection (Figure 1H). This might explain why F14 was not

1 detected in our recent quantitative proteomic analysis of VACV infection, which detected  
2 about 80% of the predicted VACV proteins [69]. Pharmacological inhibition of virus DNA  
3 replication with cytosine arabinoside (AraC) did not affect F14 protein levels, consistent with  
4 early expression, whereas late protein D8 was inhibited (Figure 1H).

5 The existence of multiple VACV inhibitors of NF- $\kappa$ B that each contribute to virulence  
6 indicates they are not redundant. To test if F14 affects NF- $\kappa$ B activation in cell culture we  
7 deleted F14 from the vv811 $\Delta$ A49 strain that lacks other known inhibitors of NF- $\kappa$ B [56] and  
8 infected an NF- $\kappa$ B firefly luciferase reporter A549 cell line [56]. As shown previously,  
9 vv811 $\Delta$ A49 inhibited NF- $\kappa$ B to a reduced extent when compared to the parental vv811 strain  
10 (Figure 1I) [56] and deletion of *F14L* reduced NF- $\kappa$ B inhibition further (Figure 1I).  
11 Immunoblotting confirmed equal infection with these viruses (Figure 1J). Notably,  
12 vv811 $\Delta$ A49 $\Delta$ F14 still suppressed NF- $\kappa$ B activation considerably, which might be explained  
13 by: (i) the existence of additional virally-encoded inhibitors that cooperate to inhibit NF- $\kappa$ B in  
14 the nucleus, or (ii) the actions of D9 and D10 decapping enzymes to reduce host mRNA [70,  
15 71].

16

#### 17 *F14 inhibits NF- $\kappa$ B at or downstream of p65*

18 To dissect how F14 functions, its impact on three hallmarks of NF- $\kappa$ B signalling were  
19 studied: namely degradation of I $\kappa$ B $\alpha$ , phosphorylation of p65 at S536 and p65 nuclear  
20 translocation. A HEK 293T-derived cell line that expresses F14 inducibly upon addition of  
21 doxycycline, was used to study the degradation of I $\kappa$ B $\alpha$ , and phosphorylation and nuclear  
22 translocation of p65 following stimulation with TNF- $\alpha$ . I $\kappa$ B $\alpha$  degradation was evident 15 min  
23 after stimulation and its re-synthesis had started by 30 min, but neither process was  
24 influenced by F14 (Figure 2A). F14 also did not affect phosphorylation of p65 at Ser<sup>536</sup>  
25 (Figure 2A) or p65 translocation into the nucleus as measured by immunofluorescence  
26 (Figure 2B). In contrast, VACV protein B14 inhibited translocation efficiently as reported [62],  
27 and VACV protein C6, an IFN antagonist [63, 68], did not (Figure 2B).

28 Next, the NF- $\kappa$ B inhibitory activity of F14 was tested by reporter gene assay following  
29 pathway activation by p65 overexpression. In contrast to B14, F14 inhibited p65-mediated  
30 activation in a dose-dependent manner without affecting p65 levels (Figure 2C). Altogether,  
31 these results showed that F14 blocks NF- $\kappa$ B in the nucleus at or downstream of p65. F14  
32 thus fits the criteria described previously for the unknown inhibitor of NF- $\kappa$ B encoded by  
33 VACV and expressed by vv811 $\Delta$ A49 [56].

34

#### 35 *F14 orthologues are conserved in orthopoxviruses and mimic the p65 transactivation domain*

36 Poxvirus immunomodulatory proteins are generally encoded in the variable genome termini,  
37 rather than the central part of the genome that encodes proteins for virus replication, share  
38 lower sequence identity and show genus-specific distribution [61]. Even among  
39 orthopoxviruses, only a few of the immunomodulatory genes are present in all virus species  
40 [61]. Nonetheless, Viral Orthologous Clusters [72] and protein BLAST searches found  
41 orthologues of VACV F14 in all orthopoxviruses, with 70.7% to 98.6% amino acid (aa)  
42 identity (Figure 3A). The C-terminal half of F14 was more conserved and included a  
43 predicted coiled-coil region (aa 34-47), the only structural motif predicted via bioinformatic  
44 analyses. However, the Phyre2 algorithm [73] predicted the C-terminal aa 55 to 71 to adopt  
45 an  $\alpha$ -helical secondary structure similar to that of aa 534-546 of p65 in complex with the PH

1 domain of human general transcription factor Tfb1, or aa 534-550 of p65 in complex with the  
2 KIX domain of NF- $\kappa$ B coactivator CBP [74]. The F14 aa similarity was striking, particularly  
3 with p65 aa within a  $\phi$ xx $\phi$  $\phi$  motif essential for NF- $\kappa$ B transcription activity [74, 75]. The C  
4 terminus of p65 harbours its transactivation domain (TAD), which is divided into two  
5 subdomains that are transcriptionally independent: TA<sub>1</sub> (aa 521 to 551) and TA<sub>2</sub> (aa 428 to  
6 521) [22, 76]. TA<sub>1</sub> contributes at least 85% of p65 transcriptional activity and interacts  
7 directly with CBP [22, 74, 76]. Notably, in F14 the position equivalent to Ser<sup>536</sup> in p65, which  
8 is phosphorylated upon NF- $\kappa$ B activation [35, 39], is occupied by the negatively charged  
9 residue Asp<sup>59</sup>, a phospho-mimetic (Figure 3A).

10 These observations and the key role of CBP in NF- $\kappa$ B-dependent gene activation [20],  
11 prompted the investigation of whether F14 could interact with CBP. Immunoprecipitation (IP)  
12 of HA-tagged F14 co-precipitated CBP-FLAG from HEK 293T cells (Figure 3B). Reciprocal  
13 IP experiments showed that ectopic CBP co-precipitated F14-HA, but not GFP-HA, with or  
14 without prior TNF- $\alpha$  stimulation (Figure 3C). These interactions were also seen at  
15 endogenous levels in both HEK 293T and HeLa cells infected with vF14-TAP. F14, but not  
16 C6, co-precipitated endogenous CBP (Figure 3D).

17 To test whether the C terminus of F14 mediated transactivation via its binding to CBP, F14  
18 aa 51 to 73 were fused to the C terminus of a p65 mutant lacking the TA<sub>1</sub> subdomain of the  
19 TAD ( $\Delta$ TA<sub>1</sub>) and the fusion protein was tested in a NF- $\kappa$ B luciferase reporter gene assay.  
20 Compared to wildtype p65, the p65 $\Delta$ TA<sub>1</sub> mutant was impaired in its transactivating activity,  
21 which was restored to wildtype levels upon fusion to F14<sub>51-73</sub> (Figure 3E). This result argues  
22 strongly that the C terminus of F14 mimics the TA<sub>1</sub> of p65 and this mimicry might explain  
23 how F14 inhibits NF- $\kappa$ B activation.

24

#### 25 *F14 outcompetes NF- $\kappa$ B for binding to CBP*

26 The similarity between the C termini of F14 and p65 led us to investigate if the conserved aa  
27 contributed to the NF- $\kappa$ B inhibitory activity of F14. Based on the structure of CBP KIX  
28 domain in complex with p65 TA<sub>1</sub> [74], residues of F14 TAD-like domain corresponding to  
29 residues of p65 important for its binding to CBP were mutated. Three sites were altered by  
30 site-directed mutagenesis of F14: the dipeptide Asp<sup>62/63</sup>, and the following Leu<sup>65</sup> and Leu<sup>68</sup>  
31 of the  $\phi$ xx $\phi$  $\phi$  motif. F14 L65A or L68A still inhibited NF- $\kappa$ B efficiently (Figure 4A). In contrast,  
32 mutation of Asp<sup>62/63</sup> to either alanine (D62/63A) or lysine (D62/63K) abolished the inhibitory  
33 activity (Figure 4A). Protein expression was comparable across the different F14 mutants  
34 (Figure 4A). The loss of NF- $\kappa$ B inhibitory activity of D62/63A and D62/63K mutants  
35 correlated with their reduced capacity to co-precipitate CBP, whereas L65A and L68A  
36 mutants co-precipitated CBP to the same extent as wildtype F14 (Figure 4B). The mutation  
37 of the negatively charged Asp<sup>62/63</sup> to positively charged Lys residues was more efficient in  
38 disrupting the interaction between F14 and CBP than only abolishing the charge (Figure 4B).  
39 Collectively, these results highlight the importance of the negatively charged dipeptide  
40 Asp<sup>62/63</sup> within the TAD-like domain for NF- $\kappa$ B inhibition by F14.

41 Next we tested if F14 could disrupt the interaction of p65 with its coactivator CBP [20]. HEK  
42 293T cells were transfected with vectors expressing p65 and CBP or RIG-I, and VACV  
43 proteins F14 or C6. The amount of p65-HA immunoprecipitated by ectopic CBP was reduced  
44 by increasing amounts of F14 but not C6 (Figure 5A, B). Quantitative analysis showed  
45 equivalent ectopic CBP immunoprecipitation with or without F14 (Figure 5C). Furthermore,  
46 the mutation D62/63K diminished the capacity of F14 to disrupt the interaction of CBP and

1 p65 (Figure 5D). This observation correlated well with the reduced capacity of the D62/63K  
2 mutant to co-precipitate CBP (Figure 4B).

3

#### 4 *F14 suppresses expression of a subset of NF-κB-responsive genes*

5 To address the impact of F14 on the induction of endogenous NF-κB-responsive genes by  
6 TNF-α, the T-REx-293 cell lines inducibly expressing F14 or C6 were utilised (Figure 6G).  
7 NF-κB-responsive genes display different temporal kinetics upon activation, with “early” gene  
8 transcripts peaking between 30 – 60 min after stimulation before declining, whilst “late” gene  
9 transcripts accumulate slowly and progressively, peaking 3 h post stimulation [15, 16]. In  
10 F14-expressing cells, mRNAs of *NFKBIA* and *CXCL8* “early” genes had equivalent induction  
11 kinetics compared to C6-expressing cells (Figure 6A, B). The lack of inhibition of F14 on the  
12 expression of *NFKBIA* mRNA is in agreement with the previous finding that the re-synthesis  
13 of IκBα (*NFKBIA* protein product) is unaffected by F14 after its proteasomal degradation  
14 induced by TNF-α (Figure 2A). Conversely, F14 inhibited the accumulation of the mRNAs of  
15 *CCL2* and *CXCL10* “late” genes in response to TNF-α (Figure 6D, E).

16 *CXCL8* and *CXCL10* encode chemokines CXCL8 and CXCL10 (also known as IL-8 and IP-  
17 10, respectively) that are secreted from stimulated cells. Following induction of VACV  
18 protein expression (Figure 6H) the levels of these chemokines were measured by ELISA and  
19 showed that secretion of CXCL10, but not CXCL8, was inhibited by F14. In contrast, the  
20 secretion of both chemokines was inhibited, or unaffected, by VACV proteins B14 or C6,  
21 respectively, as expected (Figure 6C, F). An inhibitor of IKKβ, B14 inhibited the secretion of  
22 chemokines, whereas C6, an inhibitor of IRF3 and type I IFN signalling, had a negligible  
23 effect (Figure 6C, F). Thus, unlike other VACV NF-κB inhibitors, F14 inhibits only a subset of  
24 NF-κB-responsive genes.

25

#### 26 *Acetylation of p65 and recruitment of BRD4 are inhibited by F14*

27 Posttranslational modifications of p65 accompany NF-κB translocation to the nucleus and  
28 some, such as acetylation by acetyltransferases CBP and p300, are associated with  
29 increased transcriptional activity [[36, 37, 39]; reviewed by [13, 33, 34]]. F14 did not interfere  
30 with the phosphorylation of p65 at Ser<sup>536</sup> (Figure 2A), and so the acetylation of p65 Lys<sup>310</sup>,  
31 was investigated. T-REx-293 cell lines that inducibly express F14 or contain the empty  
32 vector (EV) control were transfected with plasmids expressing p65 and CBP in the presence  
33 of the inducer, doxycycline. Although both cell lines expressed equivalent amounts of ectopic  
34 p65 and CBP, the amount of p65 acetylated at Lys<sup>310</sup> was greatly diminished by F14 (Figure  
35 7A). Quantitative analysis showed acetylated p65 was reduced 90% by F14 (Figure 7B).  
36 This result, together with the results presented in Figure 5, indicated that the reduced  
37 acetylation of p65 was due to disruption of the interaction between p65 and CBP by F14.

38 BRD4 docks onto acetylated histones and non-histone proteins and recruits transcriptional  
39 regulatory complexes to the chromatin [reviewed by [77]]. For instance, acetylated Lys<sup>310</sup> on  
40 p65 serves as a docking site for the bromodomains 1 and 2 of BRD4, which then recruits P-  
41 TEFb to promote RNAP II elongation during transcription of some NF-κB-responsive genes  
42 [40]. The differential sensitivity of TNF-α-stimulated genes to the inhibition of NF-κB by F14  
43 might reflect the differential requirement of p65 acetylated at Lys<sup>310</sup>, and the subsequent  
44 recruitment of BRD4, to activate the expression from NF-κB-responsive promoters [40]. This  
45 hypothesis was tested by chromatin immunoprecipitation with an anti-BRD4 antibody



1 followed by quantitative PCR of the promoters of two representative genes: *NFKBIA*,  
2 insensitive to F14 inhibition, and *CXCL10*, sensitive to inhibition. BRD4 was recruited to both  
3 promoters after TNF- $\alpha$  stimulation, with BRD4 present on *NFKBIA* promoter at 1 and 5 h  
4 post-stimulation, whereas BRD4 was evident on *CXCL10* promoter only at 5 h post-  
5 stimulation, mirroring the kinetics of mRNA accumulation (Figure 7C; see Figure 6E). In the  
6 presence of F14, the recruitment of BRD4 to *NFKBIA* promoter remained unaffected, whilst  
7 its recruitment to *CXCL10* was blocked (Figure 7C). This strongly suggests that inhibition of  
8 acetylation of p65 at Lys<sup>310</sup> by F14 is relayed downstream to the recruitment of BRD4 to the  
9 “F14-sensitive” *CXCL10* promoter, but not to the “F14-insensitive” *NFKBIA* promoter.

10

### 11 *F14 is a unique viral antagonist of NF- $\kappa$ B*

12 The TAD domain of p65 belongs to the class of acidic activation domains, characterised by a  
13 preponderance of Asp or Glu residues surrounding hydrophobic motifs [22]. VP16 is a  
14 transcriptional activator from herpes simplex virus (HSV) type 1 that bears a prototypical  
15 acidic TAD (Figure 8A) and inhibits the expression of virus-induced IFN- $\beta$  by association with  
16 p65 and IRF3 [78]. Although the VP16-mediated inhibition of the IFN- $\beta$  promoter was  
17 independent of its TAD, we revisited this observation to investigate the effect of VP16 more  
18 specifically on NF- $\kappa$ B-dependent gene activation. VP16 inhibited NF- $\kappa$ B reporter gene  
19 expression in a dose-dependent manner and deletion of the TAD reduced NF- $\kappa$ B inhibitory  
20 activity of VP16 about 2-fold, but some activity remained (Figure 8A).

21 A search for other viral proteins that contain motifs resembling the  $\phi$ xx $\phi$  motif present in  
22 acidic transactivation activation domains detected a divergent  $\phi$ xx $\phi$  motif in the protein E7  
23 (aa 79-83) from the high-risk human papillomavirus (HPV) 16, with acidic residues upstream  
24 (Asp<sup>75</sup>) or within (Glu<sup>80</sup> and Asp<sup>81</sup>) the motif (Figure 8B). E7 has been reported to inhibit NF-  
25  $\kappa$ B activation, in addition to its role in promoting cell cycle progression [79-82]. We confirmed  
26 that HPV-16 protein E7 inhibits NF- $\kappa$ B-dependent gene expression, albeit to a lesser extent  
27 than VACV F14 or HSV-1 VP16 (Figure 8B). Furthermore, E7 mutants harbouring aa  
28 substitutions that inverted the charge of Asp<sup>75</sup> (D75K) or added a positive charge to the  
29 otherwise hydrophobic Leu<sup>83</sup> (L83R) were impaired in their capacity to inhibit NF- $\kappa$ B (Figure  
30 8B).

31 Lastly, the ability of VP16 and E7 to associate with CBP was assessed after ectopic  
32 expression in HEK 293T cells. Neither VP16 nor E7, like VACV protein C6 used as negative  
33 control, co-precipitated CBP under conditions in which F14 did (Figure 8C). These findings  
34 indicate that the mimicry of p65 TAD by F14 is a strategy unique among human pathogenic  
35 viruses to suppress the activation of NF- $\kappa$ B.

36

## 1 DISCUSSION

2 The inducible transcription of NF- $\kappa$ B-dependent genes is a critical response to virus  
3 infection. After binding to  $\kappa$ B sites in the genome, NF- $\kappa$ B promotes the recruitment of  
4 chromatin remodelling factors, histone-modifying enzymes, and components of the  
5 transcription machinery to couple the sensing of viral and inflammatory signals to the  
6 selective activation of the target genes. In response, viruses have evolved multiple evasion  
7 strategies, including interference with NF- $\kappa$ B activation. VACV is a paradigm in viral evasion  
8 mechanisms, inasmuch as this poxvirus encodes 15 proteins known to intercept the  
9 signalling cascades downstream of PRRs and cytokine receptors that activate NF- $\kappa$ B  
10 [reviewed by [50, 51], [83, 84]]. Nonetheless, a VACV strain lacking all these inhibitors still  
11 prevented NF- $\kappa$ B activation after p65 translocation into the nucleus [56] indicating the  
12 existence of other inhibitor(s).

13 Here VACV protein F14 is shown to inhibit NF- $\kappa$ B activation within the nucleus and its  
14 mechanism of action is elucidated. First, ectopic expression of F14 reduces NF- $\kappa$ B-  
15 dependent gene expression stimulated by TNF- $\alpha$  or IL-1 $\beta$  (Figure 1A, B). Second, F14 is  
16 expressed early during VACV infection, and is small enough (8 kDa) to diffuse passively into  
17 the nucleus after expression in cytoplasmic viral factories (Figure 1E, H). Third, a VACV  
18 strain lacking both A49 and F14 (vv811 $\Delta$ A49 $\Delta$ F14) is less able to suppress cytokine-  
19 stimulated NF- $\kappa$ B-dependent gene expression than vv811 $\Delta$ A49 (Figure 1I). Fourth, following  
20 TNF- $\alpha$  stimulation, I $\kappa$ B $\alpha$  degradation, IKK-mediated phosphorylation of p65 at Ser<sup>536</sup> and p65  
21 accumulation in the nucleus remained unaffected in the presence of F14 (Figure 2A, B). And  
22 fifth, F14 blocked NF- $\kappa$ B-dependent gene expression stimulated by p65 overexpression,  
23 indicating that it acts at or downstream of p65 (Figure 2C). Lastly, despite the presence of  
24 several other VACV encoded NF- $\kappa$ B inhibitors, the biological importance of F14 was  
25 illustrated by its contribution to virulence (Figure 1F, G), a feature shared with many  
26 immunomodulatory proteins from VACV, including some inhibitors of NF- $\kappa$ B [reviewed by  
27 [50, 51]].

28 Mechanistically, F14 inhibits NF- $\kappa$ B via a C-terminal 23 aa motif, resembling p65 acidic  
29 activation domain, which disrupts the binding of p65 to its coactivator CBP (Figures 4 and 5).  
30 Consequently, F14 reduces acetylation of p65 Lys<sup>310</sup> and subsequent recruitment of BRD4  
31 to the *CXCL10* promoter, but not to the *NFKBIA* promoter (Figure 7). These findings  
32 correlated with F14 suppressing *CXCL10* (and *CCL2*), but not *NFKBIA* (and *CXCL8*), mRNA  
33 expression (Figure 6A, B, D, E). The selective inhibition of a subset of NF- $\kappa$ B-dependent  
34 genes by F14, despite the interference with molecular events deemed important for p65-  
35 mediated transactivation, underscores the complexity of the nuclear actions of NF- $\kappa$ B. Initial  
36 understanding of NF- $\kappa$ B-mediated gene activation was derived mostly using artificial reporter  
37 plasmids, but subsequent genome-wide, high-throughput studies uncovered diverse  
38 mechanisms of gene activation [14, 16, 24, 29, 30, 85, 86]. Because multiple promoters  
39 containing  $\kappa$ B sites are preloaded with CBP/p300, RNAP II and general transcription factors,  
40 the activation of transcription by NF- $\kappa$ B relies on the recruitment of BRD4 [85, 86].

41 Recruitment of BRD4 to the promoters and enhancers occurs via bromodomain-mediated  
42 docking onto acetylated lysine residues on either histones or non-histone proteins and  
43 promotes RNAP II processivity [reviewed by [77]]. BRD4 is recruited to NF- $\kappa$ B-bound  
44 promoters via the recognition of p65 acetylated at Lys<sup>310</sup> [40]. This explains the observation  
45 that BRD4 is less enriched on the *CXCL10* promoter following TNF- $\alpha$  stimulation in the  
46 presence of F14, which is associated with the reduced acetylation of p65 by CBP (Figure 7A,  
47 B, D). Nonetheless, BRD4 enrichment on *NFKBIA* promoter remained unaffected in the  
48 presence of F14 (Figure 7C), suggesting the existence of alternative mechanisms of BRD4

1 recruitment to the promoter of NF- $\kappa$ B-responsive genes. It is possible that acetylated  
2 histones mediate BRD4 recruitment to some NF- $\kappa$ B-bound promoters in the absence of  
3 acetylated p65. For instance, histone 4 acetylated on Lys<sup>5</sup>, Lys<sup>8</sup> and Lys<sup>12</sup> (H4K5/K8/K12ac)  
4 is responsible for BRD4 recruitment to NF- $\kappa$ B-responsive genes upon lipopolysaccharide  
5 stimulation [85]. Alternatively, the genes whose expression is insensitive to F14 might be  
6 activated independently of the p65 TA<sub>1</sub> domain, as it is the case of some NF- $\kappa$ B-responsive  
7 genes in mouse fibroblasts stimulated with TNF- $\alpha$ , including *Nfkb1a*. For those genes, p65  
8 occupancy on the promoter elements suffices for gene activation, via recruitment of  
9 secondary transcription factors [24].

10 In the nucleus, p65 engages with multiple binding partners via its transactivation domains,  
11 including the direct interactions between TA<sub>1</sub> and TA<sub>2</sub> and the KIX and transcriptional  
12 adaptor zinc finger (TAZ) 1 domains of CBP, respectively. These interactions are mediated  
13 by hydrophobic contacts of the  $\phi$ xx $\phi$  motifs and complemented by electrostatic contacts by  
14 the acidic residues surrounding the hydrophobic motifs [74, 86]. Sequence analysis  
15 suggested that F14 mimics the p65 TA<sub>1</sub> domain (Figure 3A). Indeed, fusion of the TAD-like  
16 domain of F14 to a p65 mutant lacking the TA<sub>1</sub> domain restored its transactivation activity to  
17 wildtype levels (Figure 3E). This explains a rather spurious observation from a yeast two-  
18 hybrid screen of VACV protein-protein interactions, in which F14 could not be tested  
19 because it was found to be a strong activator when fused to the Gal4 DNA-binding domain  
20 [87]. Site-directed mutagenesis of F14 revealed that the dipeptide Asp<sup>62/63</sup>, but not Leu<sup>65</sup> or  
21 Leu<sup>68</sup> of the  $\phi$ xx $\phi$  motif, is required for inhibition of NF- $\kappa$ B (Figure 4A), for interaction with  
22 CBP (Figure 4B) and for the efficient disruption of p65 binding to CBP (Figure 5D). This  
23 contrasts with the molecular determinants of p65 TA<sub>1</sub> binding to the KIX domain of CBP,  
24 which is dependent on the hydrophobic residues of the  $\phi$ xx $\phi$  motif, particularly Phe<sup>542</sup> [74].  
25 In the future, solving the structure of F14 TAD-like domain in complex with the KIX domain  
26 will provide insight into this discrepancy and shed light on how VACV evolved to inhibit NF-  
27  $\kappa$ B via molecular mimicry of p65 TAD. Nonetheless, the conservation of the Asp<sup>62/63</sup> site in all  
28 orthopoxvirus species (Figure 3A) implies an important function.

29 The diminished acetylation of p65 Lys<sup>310</sup> is a direct consequence of the disruption of CBP  
30 and p65 interaction by F14. Other poxvirus proteins are reported to inhibit p65 acetylation.  
31 For instance, ectopic expression of VACV protein K1 inhibited CBP-dependent p65  
32 acetylation and NF- $\kappa$ B-dependent gene expression [88], whilst during infection, K1 inhibited  
33 NF- $\kappa$ B activation upstream of I $\kappa$ B $\alpha$  degradation [89]. Regardless whether K1 inhibits NF- $\kappa$ B  
34 upstream or downstream of p65, the vv811 $\Delta$ A49 strain used to predict the existence of  
35 additional VACV inhibitors of NF- $\kappa$ B lacks K1 [56]. The other poxviral protein that inhibits  
36 CBP-mediated acetylation of p65, and thereby NF- $\kappa$ B activation, is encoded by gene 002 of  
37 orf virus, a parapoxvirus that causes mucocutaneous infections in goats and sheep [90].  
38 However, protein 002 differs from F14 in that it interacts with p65 to prevent phosphorylation  
39 at p65 Ser<sup>276</sup> and the subsequent acetylation at Lys<sup>310</sup> by p300 [90, 91].

40 F14 causes diminished p65 Lys<sup>310</sup> acetylation and consequential reduced recruitment of  
41 BRD4 to *CXCL10* promoter. The interaction between BRD4 and p65 can also reduce  
42 ubiquitylation and proteasomal degradation of nuclear p65 [92]. Thus, in addition to reducing  
43 BRD4 recruitment to the promoters of a subset of NF- $\kappa$ B-responsive genes, F14 could also  
44 destabilise nuclear p65 to terminate the pro-inflammatory signal. This represents an  
45 interesting avenue for future investigation. From the viral perspective, the selective inhibition  
46 of only a subset of NF- $\kappa$ B-responsive genes by F14 might represent an adaptation to more  
47 efficiently counteract the host immune response. If an NF- $\kappa$ B-activating signal reached the  
48 nucleus of an infected cell, maintaining expression of some NF- $\kappa$ B-dependent genes,  
49 particularly *NFKB1A*, might promote inhibition of pathway activation by I $\kappa$ B $\alpha$ . Newly

1 synthesised I $\kappa$ B $\alpha$  not only tethers cytoplasmic NF- $\kappa$ B, but can also remove NF- $\kappa$ B from the  
2 DNA and cause its export from the nucleus [17, 18, 93].

3 Our recent proteomic analysis of VACV infection revealed that both CBP and p300 are  
4 degraded in proteasome-dependent manner during infection [69]. The proteasomal  
5 degradation of CBP/p300 might be an additional immune evasion strategy of VACV, given its  
6 role in the activation of gene expression downstream of NF- $\kappa$ B and other immune signalling  
7 pathways, like IRF3 [94] and IFN-stimulated JAK/STAT [95, 96]. Because of the widespread  
8 distribution of CBP/p300-binding sites in enhancer and promoter elements across the  
9 genome, one can predict that the VACV-induced downregulation of these histone  
10 acetyltransferases will have far-reaching consequences on the host gene expression (Wang  
11 et al., 2009).

12 This study adds VACV protein F14 to the list of viral binding partners of CBP and its  
13 paralogue p300, which includes adenovirus E1A protein [97], human immunodeficiency virus  
14 (HIV) 1 Tat protein [98], human T-cell lymphotropic virus (HTLV) 1 Tax protein [99], high-risk  
15 HPV E6 protein [100], and polyomavirus T antigen [101]. Despite the fact that some of these  
16 proteins also inhibit NF- $\kappa$ B activation [79, 100, 102], F14 is unique among them in mimicking  
17 p65 TA<sub>1</sub> to bind to CBP and prevent its interaction with p65. After searching for additional  
18 viral proteins that might mimic p65 TAD, we focused on HPV E7 and HSV-1 VP16. The latter  
19 protein has a prototypical acidic TAD (Figure 8A), the former bears a motif resembling the  
20  $\phi$ xx $\phi$  motif (Figure 8B), and both proteins inhibit NF- $\kappa$ B activation [78-82]. Data presented  
21 here confirm that VP16 and, to a lesser extent, E7 each inhibit NF- $\kappa$ B-dependent gene  
22 expression (Figure 8A, B). However, neither co-precipitated CBP under conditions in which  
23 F14 did (Figure 8C), suggesting VP16 and E7 inhibit NF- $\kappa$ B activation by a mechanism  
24 distinct from F14. The interaction between VP16 and CBP is contentious [21, 78] and data  
25 presented here suggest that these two proteins do not associate with each other under the  
26 conditions tested.

27 Overall, our search for additional inhibitors of NF- $\kappa$ B activation encoded by VACV unveiled a  
28 unique viral strategy to inhibit this transcription factor that is required for the host antiviral  
29 and inflammatory responses. The detailed mechanism of how the VACV protein F14  
30 suppresses NF- $\kappa$ B activation is described. By mimicking the TA<sub>1</sub> domain of p65, F14  
31 disrupts the interaction between p65 and its coactivator CBP, thus inhibiting the downstream  
32 molecular events that trigger the activation of a subset of inflammatory genes in response to  
33 cytokine stimulation. Moreover, the contribution of F14 to virulence highlighted its  
34 physiological relevance. The molecular mimicry of F14 might be only rivalled by that of the  
35 avian reticuloendotheliosis virus, a retrovirus whose *v-Rel* gene was acquired from an avian  
36 host and modified to inhibit p65-dependent gene activation [reviewed by [103]].

37

## 1 MATERIALS AND METHODS

### 2 *Sequence analysis*

3 Candidate open reading frames (ORFs) encoding the unknown VACV inhibitor of NF- $\kappa$ B  
4 were first selected based on VACV genomes available on the NCBI database (accession  
5 numbers: NC\_006998.1 for the Western Reserve strain, and M35027.1 for the Copenhagen  
6 strain). The prediction of molecular mass and isoelectric point (pI), and of nuclear  
7 localisation signal (NLS) sequences, of the candidate VACV gene products was done with  
8 ExpASy Compute pI/MW tool ([https://web.expasy.org/compute\\_pi/](https://web.expasy.org/compute_pi/)) and SeqNLS  
9 (<http://mleg.cse.sc.edu/seqNLS/>, [104], respectively. Domain searches were performed  
10 using InterPro (<http://www.ebi.ac.uk/interpro/search/sequence/>), UniProt  
11 (<https://www.uniprot.org/uniprot/>), HHpred (<https://toolkit.tuebingen.mpg.de/tools/hhpred/>),  
12 PCOILS (<https://toolkit.tuebingen.mpg.de/tools/pcoils/>), and Phobius  
13 (<https://www.ebi.ac.uk/Tools/pfa/phobius/>) [105]. Gene family searches were done within the  
14 Pfam database (<https://pfam.xfam.org/>) and conservation within the poxvirus family, with  
15 Viral Orthologous Clusters (<https://4virology.net/virology-ca-tools/vocs/>) [72] and protein  
16 BLAST (<https://blast.ncbi.nlm.nih.gov/Blast.cgi>) searches. Phyre2  
17 (<http://www.sbg.bio.ic.ac.uk/phyre2/html/page.cgi?id=index>) [73] was used for the prediction  
18 of F14 protein structure. Multiple sequence alignments were performed using Clustal Omega  
19 (<https://www.ebi.ac.uk/Tools/msa/clustalo/>) and ESPript 3.0  
20 (<http://esprict.ibcp.fr/ESPript/ESPript/>) [106] was used for the visualisation of protein  
21 sequence alignments.

22

### 23 *Expression vectors*

24 The VACV *F14L* ORF (strain Western Reserve) was codon-optimised for expression in  
25 human cells and synthesised by GeneArt (Thermo Fisher Scientific), with an optimal 5'  
26 Kozak sequence and fused to an N-terminal FLAG epitope. For ease of subsequent  
27 subcloning, 5' BamHI and 3' XbaI restriction sites were included as well as a NotI site  
28 between the epitope tag and the ORF. For mammalian expression, N-terminal FLAG-tagged  
29 F14 was subcloned between the BamHI and XbaI restriction sites of a pcDNA4/TO vector  
30 (Invitrogen). Alternatively, codon-optimised F14 was PCR-amplified to include a 3' HA tag or  
31 a 3' FLAG or no epitope tag, and 5' BamHI and 3' XbaI sites to clone into pcDNA4/TO  
32 plasmid. In addition, codon-optimised F14 sequence was PCR-amplified to include 5' BamHI  
33 and 3' NotI sites to facilitate cloning into a pcDNA4/TO-based vector containing a TAP tag  
34 sequence after the NotI site; the TAP tag consisted of two copies of the Strep-tag II epitope  
35 and one copy of the FLAG epitope [107]. Mutant F14 expression vectors were constructed  
36 with QuikChange II XL Site-Directed Mutagenesis kit (Agilent), using primers containing the  
37 desired mutations and C-terminal TAP-tagged codon-optimised F14 cloned into pcDNA4/TO  
38 as template. Expression vectors for VACV proteins C6 and B14 have been described [64,  
39 108].

40 The ORF encoding HPV16 E7 protein was amplified from a template kindly provided by Dr.  
41 Christian Kranjec and Dr. John Doorbar (Dept. Pathology, Cambridge, UK) and cloned into  
42 5' BamHI and 3' NotI sites of a pcDNA4/TO-based vectors fused to a C-terminal TAP tag or  
43 HA epitope. Vectors expressing mutant E7 proteins were generated by site-directed  
44 mutagenesis as described above. The ORF encoding HSV-1 VP16 and  $\Delta$ TAD mutant  
45 (lacking aa 413-490) were amplified from a pEGFP-C2-based VP16 expression plasmid  
46 kindly provided by Dr. Colin Crump (Dept. Pathology, Cambridge, UK) and cloned into 5'  
47 BamHI and 3' NotI sites of a pcDNA4/TO-based vector fused to a C-terminal HA epitope.

1 Plasmids encoding TAP- and HA-tagged p65 were described elsewhere [83] and plasmids  
2 expressing FLAG-tagged mouse CBP, and HA-tagged mouse CBP were kind gift from Prof.  
3 Gerd A. Blobel (University of Pennsylvania, Philadelphia, USA) and Prof. Tony Kouzarides  
4 (Dept. Pathology and The Gurdon Institute, Cambridge, UK). Firefly luciferase reporter  
5 plasmids for NF- $\kappa$ B, ISRE and AP-1, as well as the constitutively active TK-*Renilla* luciferase  
6 reporter plasmid were kind gifts from Prof. Andrew Bowie (Trinity College, Dublin, Republic  
7 of Ireland).

8 The oligonucleotide primers used for cloning and site-directed mutagenesis are listed in  
9 Table S1. Nucleotide sequences of the inserts in all the plasmids were verified by Sanger  
10 DNA sequencing.

11

## 12 *Cell lines*

13 All cell lines were grown in medium supplemented with 10% foetal bovine serum (FBS, Pan  
14 Biotech), 100 units/mL of penicillin and 100  $\mu$ g/mL of streptomycin (Gibco), at 37°C in a  
15 humid atmosphere containing 5% CO<sub>2</sub>. Human embryo kidney (HEK) 293T epithelial cells,  
16 and monkey kidney BS-C-1 and CV-1 epithelial cells were grown in Dulbecco's modified  
17 Eagle's medium (DMEM, Gibco). Rabbit kidney RK13 epithelial cells were grown in minimum  
18 essential medium (MEM, Gibco) and human cervix HeLa epithelial cells, in MEM  
19 supplemented with non-essential amino acids (Gibco). T-REx-293 cells (Invitrogen) were  
20 grown in DMEM supplemented with blasticidin (10  $\mu$ g/mL, InvivoGen), whilst the growth  
21 medium of T-REx-293-derived cell lines stably transfected with pcDNA4/TO-based plasmids  
22 was further supplemented with zeocin (100  $\mu$ g/mL, Gibco).

23 The absence of mycoplasma contamination in the cell cultures was tested routinely with  
24 MycoAlert detection kit (Lonza), following the manufacturer's recommendations.

25

## 26 *Construction of recombinant viruses*

27 A VACV Western Reserve (WR) strain lacking F14 ( $\Delta$ F14) was constructed by introduction  
28 of a 137-bp internal deletion in the *F14L* ORF by transient dominant selection [109]. A DNA  
29 fragment including the first 3 bp of *F14L* ORF and 297 bp upstream, intervening NotI and  
30 HindIII sites, and the last 82 bp of the ORF and 218 bp downstream were generated by  
31 overlapping PCR and inserted into the PstI and BamHI sites of pUC13-Ecogpt-EGFP  
32 plasmid, containing the *Escherichia coli* guanylylphosphoribosyl transferase (Ecogpt) gene  
33 fused in-frame with the enhanced green fluorescent protein (EGFP) gene under the control  
34 of the VACV 7.5K promoter [68]. The resulting plasmid contained an internal deletion of the  
35 *F14L* ORF (nucleotide positions 42049-42185 from VACV WR reference genome, accession  
36 number NC\_006998.1). The remaining sequence of *F14L* was out-of-frame and contained  
37 multiple stop codons, precluding the expression of a truncated version of F14. The derived  
38 plasmid was transfected into CV-1 cells that had been infected with VACV-WR at 0.1  
39 p.f.u./cell for 1 h. After 48 h, progeny viruses that incorporated the plasmid by recombination  
40 and expressed the Ecogpt-EGFP were selected and plaque-purified three times on  
41 monolayers of BS-C-1 cells in the presence of mycophenolic acid (25  $\mu$ g/mL), supplemented  
42 with hypoxanthine (15  $\mu$ g/mL) and xanthine (250  $\mu$ g/mL). The intermediate recombinant  
43 virus was submitted to three additional rounds of plaque purification in the absence of the  
44 selecting drugs and GFP-negative plaques were selected. Under these conditions, progeny  
45 viruses can undergo a second recombination that result in loss of the Ecogpt-EGFP cassette  
46 concomitantly with either incorporation of the desired mutation ( $\Delta$ F14) or reversal to wild

1 type genotype (vF14). Because v $\Delta$ F14 and vF14 are sibling strains derived from the same  
2 intermediate virus, they are genetically identical except for the 137-bp deletion in the *F14L*  
3 locus. Viruses were analysed by PCR to identify recombinants by distinguishing wild type  
4 and  $\Delta$ F14 alleles, and the presence or absence of the EcoGpt-EGFP cassette.

5 To restore F14 expression in v $\Delta$ F14, the *F14L* locus was amplified by PCR, including about  
6 250 bp upstream and downstream of the ORF, and inserted into the PstI and BamHI sites of  
7 pUC13-EcoGpt-EGFP plasmid. Additionally, *F14L* ORF fused to the sequence coding a C-  
8 terminal TAP tag was also amplified by overlapping PCR, including the same flanking  
9 sequences described above, and inserted into the PstI and BamHI sites of pUC13-EcoGpt-  
10 EGFP plasmid. By using the same transient dominant selection method, these plasmids  
11 were used to generate two revertant strains derived from v $\Delta$ F14: (i) vF14-Rev, in which F14  
12 expression from its natural locus was restored, and (ii) vF14-TAP, expressing F14 fused to a  
13 C-terminal TAP tag under the control of its natural promoter. The vC6-TAP virus was  
14 described elsewhere [108].

15 A VACV vv811 strain lacking both A49 and F14 (vv811 $\Delta$ A49 $\Delta$ F14) was also constructed by  
16 transient dominant selection. The resultant virus contained the same 137-bp internal deletion  
17 in the *F14L* ORF within the vv811 $\Delta$ A49 strain generated previously [56]. The distinction  
18 between wild type and  $\Delta$ F14 alleles in the obtained viruses, and the presence or absence of  
19 the EcoGpt-EGFP cassette, was determined by PCR analysis.

20 The oligonucleotide primers used to generate the recombinant VACV strains are listed in  
21 Table S1. To verify that all the final recombinant viruses harboured the correct sequences,  
22 PCR fragments spanning the *F14L* locus were sequenced.

23

#### 24 *Preparation of virus stocks*

25 The stocks of virus strains derived from VACV WR were prepared in RK-13 cells. Cells  
26 grown to confluence in T-175 flasks were infected at 0.01 p.f.u./cell until complete cytopathic  
27 effect was visible. The cells were harvested by centrifugation, suspended in a small volume  
28 of DMEM supplemented with 2% FBS, and submitted to multiple cycles of freezing/thawing  
29 and sonication to lyse the cells and disrupt aggregates of virus particles and cellular debris.  
30 These crude virus stocks were used for experiments in cultured cells. Crude stocks of vv811  
31 and derived strains were prepared in the same way, except for the BS-C-1 cells used for  
32 infection. For the *in vivo* work, virus stocks were prepared by ultracentrifugation of the  
33 cytoplasmic fraction of infected cell lysates through sucrose cushion and suspension of the  
34 virus samples in 10 mM Tris-HCl pH 9.0 [110]. The viral titres in the stocks were determined  
35 by plaque assay on BS-C-1 cells.

36

#### 37 *Virus growth and spread assays*

38 To analyse virus growth properties in cell culture, single-step growth curve experiments were  
39 performed in HeLa cells. Cells were grown to about 90% confluence in T-25 flasks and then  
40 infected at 5 p.f.u./cell in growth medium supplemented with 2% FBS. Virus adsorption was  
41 at 37°C for 1 h. Then the inoculum was removed, and the cells were replenished with  
42 growth medium supplemented with 2% FBS. At 1, 8, and 24 h p.i., infected-cell supernatants  
43 and monolayers were collected for determination of extracellular and cell-associated  
44 infectious virus titres by plaque assay on BS-C-1 cells. Supernatants were clarified by  
45 centrifugation to remove cellular debris and detached cells, whereas cell monolayers were

1 scraped and disrupted by three cycles of freezing/thawing followed by sonication, to release  
2 intracellular virus particles.

3 The virus spread in cell culture was assessed by plaque formation. Confluent monolayers of  
4 BS-C-1 cells in 6-well plates were infected with 50 p.f.u./well and overlaid with MEM  
5 supplemented with 2% FBS and 1.5% carboxymethylcellulose. After 48 h, infected cell  
6 monolayers were stained with 0.5% crystal violet solution in 20% methanol and imaged.

7

#### 8 *Construction of inducible F14-expressing T-REx-293 cell line*

9 T-REx-293 cells (Invitrogen), which constitutively expresses the Tet repressor (TetR) under  
10 the control of the human cytomegalovirus (HCMV) immediate early promoter, were  
11 transfected with pcDNA4/TO-coF14-TAP plasmid, which encodes human codon-optimised  
12 F14 fused to a C-terminal TAP tag under the control of the HCMV immediate early promoter  
13 and two tetracycline operator 2 (TetO<sub>2</sub>) sites. Transfected cells were selected in the  
14 presence of blasticidin (10 µg/mL) and zeocin (100 µg/mL) and clonal cell lines were  
15 obtained by limiting dilution. Expression of protein F14 within these clones was analysed by  
16 immunoblotting and flow cytometry with anti-FLAG antibodies.

17

#### 18 *Reporter gene assays*

19 HEK 293T cells in 96-well plates were transfected in quadruplicate with firefly luciferase  
20 reporter plasmid (NF-κB, ISRE, or AP-1), TK-*Renilla* luciferase reporter plasmid (as an  
21 internal control) and the desired expression vectors or empty vector (EV) using *TransIT-LT1*  
22 transfection reagent (Mirus Bio), according to the manufacturer's instruction. On the  
23 following day, cells were stimulated with TNF-α (10 ng/ml, PeproTech) or IL-1β (20 ng/ml,  
24 PeproTech) for 8 h (for NF-κB activation), IFN-α2 (1000 U/ml, PeproTech) for 8 h (for  
25 JAK/STAT/ISRE activation), or phorbol 12-myristate 13-acetate (10 ng/ml) for 24 h (for  
26 MAPK/AP-1 activation). Alternatively, NF-κB was activated by co-transfection of p65-  
27 overexpressing plasmid and cells were harvested 24 h after transfection.

28 To measure NF-κB activation during infection, A549 cells transduced with a lentiviral vector  
29 expressing the firefly luciferase under the control of an NF-κB promoter (A549-NF-κB-Luc)  
30 [56] were grown in 96-well plates and infected with VACV vv811 and derived strains at 5  
31 p.f.u./cell. After 6 h, cells were stimulated with TNF-α (10 ng/ml, PeproTech) or IL-1β (20  
32 ng/ml, PeproTech) for an additional 6 h. In parallel, A549-NF-κB-Luc cells grown in 6-well  
33 plates were infected with the equivalent amount of virus for 12 h and cell lysates were  
34 analysed by immunoblotting.

35 Cells were lysed using passive lysis buffer (Promega) and firefly and *Renilla* luciferase  
36 luminescence was measured using a FLUOstar luminometer (BMG). Promoter activity was  
37 obtained by calculation of firefly/*Renilla* luciferase ratios and the promoter activity under  
38 pathway stimulation was normalised to the activity of the respective non-stimulated control of  
39 each protein under test. In parallel, aliquots of the replicas of each condition tested were  
40 combined, mixed with 5 × SDS-polyacrylamide gel loading buffer, and immunoblotted to  
41 confirm the expression of the proteins tested.

42

#### 43 *Virus infection in cell culture*



1 HeLa or HEK 293T cells in 6-well plates (for protein expression analyses) or 10-cm dishes  
2 (for immunoprecipitation experiments) were infected at 5 p.f.u./cell. Viral inocula were  
3 prepared in growth medium supplemented with 2% FBS. Viral adsorption was done at 37°C  
4 for 1 h, after which the medium supplemented with 2% FBS was topped up to the  
5 appropriate vessel volume and cells were incubated at 37°C.

6

#### 7 *In vivo experiments*

8 All animal experiments were conducted according to the Animals (Scientific Procedures) Act  
9 1986 under the license PPL 70/8524. Mice were purchased from Envigo and housed in  
10 specific pathogen-free conditions in the Cambridge University Biomedical Services facility.

11 For the intradermal (i.d.) model of infection, female C57BL/6 mice (6-8-week old) were  
12 inoculated with 10<sup>4</sup> p.f.u. in both ear pinnae and the diameter of the lesion was measured  
13 daily using a micrometer [111]. For the intranasal (i.n.) model, female BALB/c mice (6-8-  
14 week old) were inoculated 5 × 10<sup>3</sup> p.f.u. divided equally into each nostril and were weighed  
15 daily [112]. In both cases, viral inocula were prepared in phosphate-buffered saline (PBS)  
16 supplemented with 0.01% bovine serum albumin (BSA, Sigma Aldrich) and the infectious  
17 titres in the administered inocula were confirmed by plaque assay.

18 For quantification of virus replication after the i.d. infection, infected mice were culled 3, 7,  
19 and 10 d p.i. and ear tissues were collected, homogenised and passed through a 70-µm  
20 nylon mesh using DMEM containing 10% FBS. Samples were frozen and thawed three  
21 times, sonicated thoroughly to liberate cell-associated virus particles, and the infectious titres  
22 present were determined by plaque assay on BS-C-1 cells.

23

#### 24 *Immunoblotting*

25 For analysis of protein expression, cells were washed with ice-cold PBS and lysed on ice  
26 with cell lysis buffer [50 mM Tris-HCl pH 8.0, 150 mM NaCl, 1 mM EDTA, 10% (v/v) glycerol,  
27 1% (v/v) Triton X-100 and 0.05% (v/v) Nonidet P-40 (NP-40)], supplemented with protease  
28 (cOmplete Mini, Roche) and phosphatase inhibitors (PhosSTOP, Roche), for 20 min. Lysed  
29 cells were scraped and lysates were clarified to remove insoluble material by centrifugation  
30 at 17,000 × g for 15 min at 4°C. Protein concentration in the cell lysate was determined  
31 using a bicinchoninic acid protein assay kit (Pierce). After mixing with 5 × SDS-gel loading  
32 buffer and boiling at 100°C for 5 min, equivalent amounts of protein samples were loaded  
33 onto SDS-polyacrylamide gels or NuPAGE 4 to 12% Bis-Tris precast gels (Invitrogen),  
34 separated by electrophoresis and transferred onto nitrocellulose membranes (GE  
35 Healthcare). Membranes were blocked at room temperature with either 5% (w/v) non-fat milk  
36 or 3% (w/v) BSA (Sigma Aldrich) in Tris-buffered saline (TBS) containing 0.1% (v/v) Tween-  
37 20. To detect the expression of the protein under test, the membranes were incubated with  
38 specific primary antibodies diluted in blocking buffer at 4°C overnight. After washing with  
39 TBS containing 0.1% (v/v) Tween-20, membranes were probed with fluorophore-conjugated  
40 secondary antibodies (LI-COR Biosciences) diluted in 5% (w/v) non-fat milk at room  
41 temperature for 1 h. The antibodies used for immunoblotting are listed in Table S2. After  
42 washing, membranes were imaged using the Odyssey CLx imaging system (LI-COR  
43 Biosciences), according to the manufacturer's instructions. For quantitative analysis of  
44 protein levels, the band intensities on the immunoblots were quantified using the Image  
45 Studio software (LI-COR Biosciences).

1

## 2 *Co-immunoprecipitation and pull-down assays*

3 HEK 293T or HeLa cells in 10-cm dishes were infected at 5 p.f.u./cell for 8 h or transfected  
4 overnight with the specified epitope-tagged plasmids using polyethylenimine (PEI,  
5 Polysciences, 2  $\mu$ l of 1 mg/ml stock per  $\mu$ g of plasmid DNA). For the competition assays,  
6 cells were starved of FBS for 3 h and stimulated with TNF- $\alpha$  (40 ng/ml, PeproTech) in FBS-  
7 free DMEM for 15 min before harvesting. Cells were washed twice with ice-cold PSB,  
8 scraped in immunoprecipitation (IP) buffer (50 mM Tris-HCl pH 7.4, 150 mM NaCl, 0.5%  
9 (v/v) NP-40), 0.1 mM EDTA), supplemented with protease (cOmplete Mini, Roche) and  
10 phosphatase (PhosSTOP, Roche) inhibitors, on ice, transferred to 1.5-ml microcentrifuge  
11 tubes and rotated for 30 min at 4°C. Cell lysates were centrifuged at 17,000  $\times$  g for 15 min  
12 at 4°C and the soluble fractions were incubated with 20  $\mu$ l of one of the following affinity  
13 resins equilibrated in IP buffer: (i) anti-FLAG M2 (Sigma Aldrich) for IP of FLAG- or TAP-  
14 tagged proteins; (ii) anti-HA (Sigma Aldrich) for IP of HA-tagged proteins; or (iii) Strep-Tactin  
15 Superflow resin (IBA) for pull-down of TAP-tagged protein via Strep-tag II epitope. After 2 h of  
16 rotation at 4°C, the protein-bound resins were washed three times with ice-cold IP buffer.  
17 The bound proteins were eluted by incubation with 2 $\times$  SDS-gel loading buffer and boiled at  
18 100°C for 5 min before analysis by SDS-polyacrylamide gel electrophoresis and  
19 immunoblotting, along with 10% input samples collected after clarification of cell lysates.

20

## 21 *Reverse transcription and quantitative PCR*

22 To analyse mRNA expression of NF- $\kappa$ B-responsive genes, T-REx-293-F14 and T-REx-293-  
23 C6 cells in 12-well plates were induced overnight with 100 ng/ml doxycycline (Melford, UK)  
24 to induce the expression of the VACV proteins. The next day, cells were starved for 3 h by  
25 removal of serum from the medium and then stimulated in duplicate with TNF- $\alpha$  (40 ng/ml,  
26 PeproTech) in FBS-free DMEM for 0, 1 or 6 h. RNA was extracted using RNeasy Mini Kit  
27 (Qiagen) and complementary DNA (cDNA) was synthesised using SuperScript III reverse  
28 transcriptase (Invitrogen) and oligo-dT primers (Thermo Scientific), according to the  
29 instructions of the respective manufacturers. The mRNA levels of CCL2, CXCL8, CXCL10,  
30 GAPDH and NFKBIA were quantified by quantitative PCR using gene-specific primer sets,  
31 fast SYBR green master mix (Applied Biosystems) and the ViiA 7 real-time PCR system (Life  
32 Technologies). The oligonucleotide primers used for the qPCR analysis of gene expression  
33 are listed in Table S1. Fold-induction of the NF- $\kappa$ B-responsive genes was calculated by the  
34  $2^{-\Delta\Delta C_t}$  method using non-stimulated T-REx-293-C6 as the reference sample and *GAPDH* as  
35 the housekeeping control gene.

36

## 37 *Enzyme-linked immunosorbent assay (ELISA)*

38 The secretion of CXCL8 and CXCL10 was measured by ELISA. T-REx-293-EV, T-REx-293-  
39 B14, T-REx-293-C6 and T-REx-293-F14 cells in 12-well plates were incubated overnight in  
40 the presence or absence of 100 ng/ml doxycycline (Melford, UK) to induce VACV protein  
41 expression. The next day, cells were stimulated in triplicate with TNF- $\alpha$  (40 ng/ml,  
42 PeproTech) in DMEM supplemented with 2% FBS for 16 h. The supernatants were assayed  
43 for human CXCL8 and CXCL10 using the respective DuoSet ELISA kits (R&D Biosystems),  
44 according to the manufacturer's instructions.

45

## 1 *Immunofluorescence*

2 For immunofluorescence microscopy, T-REx-293-EV, T-REx-293-B14, T-REx-293-C6 and  
3 T-REx-293-F14 cells on poly-D-lysine-treated glass coverslips placed inside 6-well plates.  
4 Following induction of protein expression with 100 ng/ml doxycycline (Melford, UK)  
5 overnight, cells were starved of serum for 3 h and then stimulated with 40 ng/ml TNF- $\alpha$   
6 (PeproTech) in FBS-free DMEM for 15 min. At the moment of harvesting, the cells were  
7 washed twice with ice-cold PBS and fixed in 4% (v/v) paraformaldehyde. After quenching of  
8 free formaldehyde with 150 mM ammonium chloride, the fixed cells were permeabilised with  
9 0.1% (v/v) Triton X-100 in PBS and blocked with 10% (v/v) FBS in PBS. Antibody staining  
10 was carried out with mouse anti-p65 (Santa Cruz) and rabbit anti-FLAG (Sigma Aldrich)  
11 antibodies for 1 h, followed by incubation with the appropriate AlexaFluor fluorophore-  
12 conjugated secondary antibodies (Invitrogen Molecular Probes) and mounting onto glass  
13 slides with Mowiol 4-88 (Calbiochem) containing 0.5  $\mu$ g/ml DAPI (4',6-diamidino-2-  
14 phenylindole, Sigma Aldrich). The antibodies used for immunofluorescence are listed in  
15 Table S2. Images were acquired on an LSM 700 confocal microscope (Zeiss) using ZEN  
16 system software (Zeiss). Quantification of nuclear localisation of p65 was done manually on  
17 the ZEN lite (blue edition, Zeiss).

18

## 19 *Chromatin immunoprecipitation and quantitative PCR (ChIP-qPCR)*

20 T-REx-F14 cells in 15-cm dishes were incubated overnight in the absence or in the presence  
21 of 100 ng/ml doxycycline (Melford, UK) to induce F14 expression. The next day, cells were  
22 starved of FBS for 3 h and stimulated with TNF- $\alpha$  (40 ng/ml, PeproTech) in FBS-free DMEM  
23 for 0, 1 or 5 h. Cells were crosslinked with 1% (v/v) formaldehyde added directly to the  
24 growth medium. After 10 min at room temperature, crosslinking was stopped by the  
25 addition of 0.125 M glycine. Cells were then lysed in 0.2% NP-40, 10 mM Tris-HCl pH 8.0,  
26 10 mM NaCl, supplemented with protease (cOmplete Mini, Roche), phosphatase  
27 (PhosSTOP, Roche) and histone deacetylase (10 mM sodium butyrate, Sigma Aldrich)  
28 inhibitors, and nuclei were recovered by centrifugation at 600  $\times$  g for 5 min at 4°C. To  
29 prepare the chromatin, nuclei were lysed in 1% (w/v) SDS, 50 mM Tris-HCl pH 8.0,  
30 10 mM EDTA, plus protease/phosphatase/histone acetylase inhibitors, and lysates were  
31 sonicated in a Bioruptor Pico (Diagenode) to achieve DNA fragments of about 500 bp. After  
32 sonication, samples were centrifuged at 3,500  $\times$  g for 10 min at 4°C and supernatants were  
33 diluted four-fold in IP dilution buffer [20 mM Tris-HCl pH 8.0, 150 mM NaCl, 2 mM EDTA, 1%  
34 (v/v) Triton X-100, 0.01% (w/v) SDS] supplemented with protease/phosphatase/histone  
35 acetylase inhibitors.

36 Protein G-conjugated agarose beads (GE Healthcare) equilibrated in IP dilution buffer were  
37 used to preclear the chromatin for 1 h at 4°C with rotation. Before the immunoprecipitation,  
38 20% of the precleared chromatin was kept as input control. Immunoprecipitation was  
39 performed with 8  $\mu$ g of anti-BRD4 antibody (Cell Signalling Technology, #13440) or anti-GFP  
40 (Abcam, #ab290), used as negative IgG control, overnight 4°C with rotation. Protein-DNA  
41 immunocomplexes were retrieved by incubation with 60  $\mu$ l of equilibrated protein G-  
42 conjugated agarose beads (GE Healthcare), for 2 h at 4°C, followed by centrifugation at  
43 5,000  $\times$  g for 2 min at 4°C. Immunocomplex-bound beads were then washed: (i) twice with  
44 IP wash I [20 mM Tris-HCl pH 8.0, 50 mM NaCl, 2 mM EDTA, 1% (v/v) Triton X-100, 0.1%  
45 (w/v) SDS]; (ii) once with IP wash buffer II [10 mM Tris-HCl pH 8.0, 250 mM LiCl, 1 mM  
46 EDTA, 1% (v/v) NP-40, 1% (w/v) sodium deoxycholate]; and (iii) twice with TE buffer (10 mM  
47 Tris-HCl pH 8.0, 1 mM EDTA). Antibody-bound chromatin was eluted with 1% SDS, 100 mM

1 sodium bicarbonate for 15 min at room temperature. Formaldehyde crosslinks were reversed  
2 by incubation overnight at 67°C in presence of 1 µg of RNase A and 300 mM NaCl, followed  
3 by proteinase K digestion for 2 h at 45°C. Co-immunoprecipitated DNA fragments were  
4 purified using the QIAquick PCR purification kit (Qiagen) and analysed by quantitative PCR  
5 targeting the promoter elements of *NFKBIA* and *CXCL10* containing κB sites. The  
6 oligonucleotide primers used for the qPCR analysis of ChIP are listed in Table S1. For  
7 display of the ChIP-qPCR data, the signals obtained from the ChIP with each antibody were  
8 divided by the signals obtained from the corresponding input sample.

9

#### 10 *Statistical analysis*

11 Experimental data are presented as means + s.d. or means ± s.e.m. for *in vivo* results,  
12 unless otherwise stated in figure legends. Statistical significance was calculated by two-  
13 tailed unpaired Student's *t*-test. GraphPad Prism software (version 8.4.2) was used for  
14 statistical analysis.

15

1 ACKNOWLEDGEMENTS

2 The authors thank Rachel Seear, Stephanie Macilwee, and Jemma Milburn for technical  
3 support. We also thank John Doorbar (Dept. Pathology, University of Cambridge, UK), Colin  
4 Crump (Dept. Pathology, University of Cambridge, UK), Tony Kouzarides (Dept. Pathology  
5 and The Gurdon Institute, University of Cambridge, UK), and Gerd Blobel (University of  
6 Pennsylvania, Philadelphia, USA) for providing us with reagents. We are also grateful to  
7 Tony Kouzarides for helpful advice and to Callum Talbot-Cooper for critical reading of the  
8 manuscript.

9

10 FUNDING

11 This work was supported by grant 090315 from the Wellcome Trust (to G.L.S.). J.D.A. was a  
12 postdoctoral fellow of the Science without Borders programme from CNPq-Brazil (grant  
13 235246/2014-0).

14

15 AUTHOR CONTRIBUTION

16 Conceptualisation: JDA, AAT, GLS

17 Methodology: JDA, HR, AAT, EVS, CAM, AJB

18 Software: N/A

19 Validation: JDA, HR, AAT, EVS

20 Formal Analysis: JDA, HR

21 Investigation: JDA, HR, AAT, EVS

22 Resources: AAT, CAM, AJB, GLS

23 Data Curation: JDA

24 Writing – Original Draft Preparation: JDA

25 Writing – Review and Editing: JDA, HR, AAT, CAM, AJB, GLS

26 Visualisation: JDA

27 Supervision: JDA, GLS

28 Project Administration: JDA, GLS

29 Funding: JDA, GLS

30

## 1 REFERENCES

- 2 1. Elde, N.C., et al., *Protein kinase R reveals an evolutionary model for defeating viral mimicry*.  
3 Nature, 2009. **457**(7228): p. 485-9.
- 4 2. Hancks, D.C., et al., *Overlapping Patterns of Rapid Evolution in the Nucleic Acid Sensors cGAS  
5 and OAS1 Suggest a Common Mechanism of Pathogen Antagonism and Escape*. PLoS Genet,  
6 2015. **11**(5): p. e1005203.
- 7 3. Alves, J.M., et al., *Parallel adaptation of rabbit populations to myxoma virus*. Science, 2019.  
8 **363**(6433): p. 1319-1326.
- 9 4. Medzhitov, R., *Recognition of microorganisms and activation of the immune response*.  
10 Nature, 2007. **449**(7164): p. 819-26.
- 11 5. Iwasaki, A., *A virological view of innate immune recognition*. Annu Rev Microbiol, 2012. **66**:  
12 p. 177-96.
- 13 6. Griffith, J.W., C.L. Sokol, and A.D. Luster, *Chemokines and chemokine receptors: positioning  
14 cells for host defense and immunity*. Annu Rev Immunol, 2014. **32**: p. 659-702.
- 15 7. Netea, M.G., et al., *A guiding map for inflammation*. Nat Immunol, 2017. **18**(8): p. 826-831.
- 16 8. Altan-Bonnet, G. and R. Mukherjee, *Cytokine-mediated communication: a quantitative  
17 appraisal of immune complexity*. Nat Rev Immunol, 2019. **19**(4): p. 205-217.
- 18 9. Bonilla, F.A. and H.C. Oettgen, *Adaptive immunity*. J Allergy Clin Immunol, 2010. **125**(2 Suppl  
19 2): p. S33-40.
- 20 10. Hayden, M.S. and S. Ghosh, *Signaling to NF-kappaB*. Genes Dev, 2004. **18**(18): p. 2195-224.
- 21 11. Vallabhapurapu, S. and M. Karin, *Regulation and function of NF-kappaB transcription factors  
22 in the immune system*. Annu Rev Immunol, 2009. **27**: p. 693-733.
- 23 12. Brubaker, S.W., et al., *Innate immune pattern recognition: a cell biological perspective*. Annu  
24 Rev Immunol, 2015. **33**: p. 257-90.
- 25 13. Chen, L.F. and W.C. Greene, *Shaping the nuclear action of NF-kappaB*. Nat Rev Mol Cell Biol,  
26 2004. **5**(5): p. 392-401.
- 27 14. Kaikkonen, M.U., et al., *Remodeling of the enhancer landscape during macrophage  
28 activation is coupled to enhancer transcription*. Mol Cell, 2013. **51**(3): p. 310-25.
- 29 15. Tian, B., D.E. Nowak, and A.R. Brasier, *A TNF-induced gene expression program under  
30 oscillatory NF-kappaB control*. BMC Genomics, 2005. **6**: p. 137.
- 31 16. Zhao, M., et al., *Transcriptional outcomes and kinetic patterning of gene expression in  
32 response to NF-kappaB activation*. PLoS Biol, 2018. **16**(9): p. e2006347.
- 33 17. Huang, T.T., et al., *A nuclear export signal in the N-terminal regulatory domain of  
34 IkkappaBalpha controls cytoplasmic localization of inactive NF-kappaB/IkkappaBalpha  
35 complexes*. Proc Natl Acad Sci U S A, 2000. **97**(3): p. 1014-9.
- 36 18. Johnson, C., D. Van Antwerp, and T.J. Hope, *An N-terminal nuclear export signal is required  
37 for the nucleocytoplasmic shuttling of IkkappaBalpha*. EMBO J, 1999. **18**(23): p. 6682-93.
- 38 19. Barboric, M., et al., *NF-kappaB binds P-TEFb to stimulate transcriptional elongation by RNA  
39 polymerase II*. Mol Cell, 2001. **8**(2): p. 327-37.
- 40 20. Gerritsen, M.E., et al., *CREB-binding protein/p300 are transcriptional coactivators of p65*.  
41 Proc Natl Acad Sci U S A, 1997. **94**(7): p. 2927-32.
- 42 21. Naar, A.M., et al., *Composite co-activator ARC mediates chromatin-directed transcriptional  
43 activation*. Nature, 1999. **398**(6730): p. 828-32.
- 44 22. Schmitz, M.L., et al., *Interaction of the COOH-terminal transactivation domain of p65 NF-  
45 kappa B with TATA-binding protein, transcription factor IIB, and coactivators*. J Biol Chem,  
46 1995. **270**(13): p. 7219-26.
- 47 23. Sheppard, K.A., et al., *Transcriptional activation by NF-kappaB requires multiple coactivators*.  
48 Mol Cell Biol, 1999. **19**(9): p. 6367-78.
- 49 24. van Essen, D., et al., *Two modes of transcriptional activation at native promoters by NF-  
50 kappaB p65*. PLoS Biol, 2009. **7**(3): p. e73.

- 1 25. Saccani, S., S. Pantano, and G. Natoli, *Modulation of NF-kappaB activity by exchange of*  
2 *dimers*. Mol Cell, 2003. **11**(6): p. 1563-74.
- 3 26. Thanos, D. and T. Maniatis, *Virus induction of human IFN beta gene expression requires the*  
4 *assembly of an enhanceosome*. Cell, 1995. **83**(7): p. 1091-100.
- 5 27. Ashall, L., et al., *Pulsatile stimulation determines timing and specificity of NF-kappaB-*  
6 *dependent transcription*. Science, 2009. **324**(5924): p. 242-6.
- 7 28. Hoffmann, A., et al., *The IkappaB-NF-kappaB signaling module: temporal control and*  
8 *selective gene activation*. Science, 2002. **298**(5596): p. 1241-5.
- 9 29. Jin, F., et al., *PU.1 and C/EBP(alpha) synergistically program distinct response to NF-kappaB*  
10 *activation through establishing monocyte specific enhancers*. Proc Natl Acad Sci U S A, 2011.  
11 **108**(13): p. 5290-5.
- 12 30. Ramirez-Carrozzi, V.R., et al., *A unifying model for the selective regulation of inducible*  
13 *transcription by CpG islands and nucleosome remodeling*. Cell, 2009. **138**(1): p. 114-28.
- 14 31. Ainbinder, E., et al., *Mechanism of rapid transcriptional induction of tumor necrosis factor*  
15 *alpha-responsive genes by NF-kappaB*. Mol Cell Biol, 2002. **22**(18): p. 6354-62.
- 16 32. Saccani, S., S. Pantano, and G. Natoli, *Two waves of nuclear factor kappaB recruitment to*  
17 *target promoters*. J Exp Med, 2001. **193**(12): p. 1351-9.
- 18 33. Huang, B., et al., *Posttranslational modifications of NF-kappaB: another layer of regulation*  
19 *for NF-kappaB signaling pathway*. Cell Signal, 2010. **22**(9): p. 1282-90.
- 20 34. Perkins, N.D., *Post-translational modifications regulating the activity and function of the*  
21 *nuclear factor kappa B pathway*. Oncogene, 2006. **25**(51): p. 6717-30.
- 22 35. Sakurai, H., et al., *IkappaB kinases phosphorylate NF-kappaB p65 subunit on serine 536 in the*  
23 *transactivation domain*. J Biol Chem, 1999. **274**(43): p. 30353-6.
- 24 36. Zhong, H., R.E. Voll, and S. Ghosh, *Phosphorylation of NF-kappa B p65 by PKA stimulates*  
25 *transcriptional activity by promoting a novel bivalent interaction with the coactivator*  
26 *CBP/p300*. Mol Cell, 1998. **1**(5): p. 661-71.
- 27 37. Chen, L.F., et al., *NF-kappaB RelA phosphorylation regulates RelA acetylation*. Mol Cell Biol,  
28 2005. **25**(18): p. 7966-75.
- 29 38. Wang, Z., et al., *Genome-wide mapping of HATs and HDACs reveals distinct functions in*  
30 *active and inactive genes*. Cell, 2009. **138**(5): p. 1019-31.
- 31 39. Yang, F., et al., *IKK beta plays an essential role in the phosphorylation of RelA/p65 on serine*  
32 *536 induced by lipopolysaccharide*. J Immunol, 2003. **170**(11): p. 5630-5.
- 33 40. Huang, B., et al., *Brd4 coactivates transcriptional activation of NF-kappaB via specific binding*  
34 *to acetylated RelA*. Mol Cell Biol, 2009. **29**(5): p. 1375-87.
- 35 41. Amir-Zilberstein, L., et al., *Differential regulation of NF-kappaB by elongation factors is*  
36 *determined by core promoter type*. Mol Cell Biol, 2007. **27**(14): p. 5246-59.
- 37 42. Nowak, D.E., et al., *RelA Ser276 phosphorylation is required for activation of a subset of NF-*  
38 *kappaB-dependent genes by recruiting cyclin-dependent kinase 9/cyclin T1 complexes*. Mol  
39 Cell Biol, 2008. **28**(11): p. 3623-38.
- 40 43. Smale, S.T., *Hierarchies of NF-kappaB target-gene regulation*. Nat Immunol, 2011. **12**(8): p.  
41 689-94.
- 42 44. Peng, C., et al., *Myxoma virus M156 is a specific inhibitor of rabbit PKR but contains a loss-of-*  
43 *function mutation in Australian virus isolates*. Proc Natl Acad Sci U S A, 2016. **113**(14): p.  
44 3855-60.
- 45 45. Elde, N.C. and H.S. Malik, *The evolutionary conundrum of pathogen mimicry*. Nat Rev  
46 Microbiol, 2009. **7**(11): p. 787-97.
- 47 46. Daugherty, M.D. and H.S. Malik, *Rules of engagement: molecular insights from host-virus*  
48 *arms races*. Annu Rev Genet, 2012. **46**: p. 677-700.
- 49 47. McFadden, G., *Poxvirus tropism*. Nat Rev Microbiol, 2005. **3**(3): p. 201-13.
- 50 48. Johnston, J.B. and G. McFadden, *Poxvirus immunomodulatory strategies: current*  
51 *perspectives*. J Virol, 2003. **77**(11): p. 6093-100.

- 1 49. Seet, B.T., et al., *Poxviruses and immune evasion*. Annu Rev Immunol, 2003. **21**: p. 377-423.
- 2 50. Smith, G.L., et al., *Vaccinia virus immune evasion: mechanisms, virulence and*  
3 *immunogenicity*. J Gen Virol, 2013. **94**(Pt 11): p. 2367-2392.
- 4 51. Albarnaz, J.D., A.A. Torres, and G.L. Smith, *Modulating Vaccinia Virus Immunomodulators to*  
5 *Improve Immunological Memory*. Viruses, 2018. **10**(3).
- 6 52. Bahar, M.W., et al., *How vaccinia virus has evolved to subvert the host immune response*. J  
7 Struct Biol, 2011. **175**(2): p. 127-34.
- 8 53. Mansur, D.S., et al., *Poxvirus targeting of E3 ligase beta-TrCP by molecular mimicry: a*  
9 *mechanism to inhibit NF-kappaB activation and promote immune evasion and virulence*.  
10 PLoS Pathog, 2013. **9**(2): p. e1003183.
- 11 54. Neidel, S., et al., *Vaccinia virus protein A49 is an unexpected member of the B-cell Lymphoma*  
12 *(Bcl)-2 protein family*. J Biol Chem, 2015. **290**(10): p. 5991-6002.
- 13 55. Neidel, S., et al., *NF-kappaB activation is a turn on for vaccinia virus phosphoprotein A49 to*  
14 *turn off NF-kappaB activation*. Proc Natl Acad Sci U S A, 2019. **116**(12): p. 5699-5704.
- 15 56. Sumner, R.P., et al., *Vaccinia virus inhibits NF-kappaB-dependent gene expression*  
16 *downstream of p65 translocation*. J Virol, 2014. **88**(6): p. 3092-102.
- 17 57. Perkus, M.E., et al., *Deletion of 55 open reading frames from the termini of vaccinia virus*.  
18 Virology, 1991. **180**(1): p. 406-10.
- 19 58. Assarsson, E., et al., *Kinetic analysis of a complete poxvirus transcriptome reveals an*  
20 *immediate-early class of genes*. Proc Natl Acad Sci U S A, 2008. **105**(6): p. 2140-5.
- 21 59. Yang, Z., et al., *Simultaneous high-resolution analysis of vaccinia virus and host cell*  
22 *transcriptomes by deep RNA sequencing*. Proc Natl Acad Sci U S A, 2010. **107**(25): p. 11513-8.
- 23 60. Wenthe, S.R. and M.P. Rout, *The nuclear pore complex and nuclear transport*. Cold Spring  
24 Harb Perspect Biol, 2010. **2**(10): p. a000562.
- 25 61. Gubser, C., et al., *Poxvirus genomes: a phylogenetic analysis*. J Gen Virol, 2004. **85**(Pt 1): p.  
26 105-117.
- 27 62. Chen, R.A., et al., *Inhibition of IkappaB kinase by vaccinia virus virulence factor B14*. PLoS  
28 Pathog, 2008. **4**(2): p. e22.
- 29 63. Stuart, J.H., et al., *Vaccinia Virus Protein C6 Inhibits Type I IFN Signalling in the Nucleus and*  
30 *Binds to the Transactivation Domain of STAT2*. PLoS Pathog, 2016. **12**(12): p. e1005955.
- 31 64. Torres, A.A., et al., *Multiple Bcl-2 family immunomodulators from vaccinia virus regulate*  
32 *MAPK/AP-1 activation*. J Gen Virol, 2016. **97**(9): p. 2346-2351.
- 33 65. Yang, Z., et al., *Deciphering poxvirus gene expression by RNA sequencing and ribosome*  
34 *profiling*. J Virol, 2015. **89**(13): p. 6874-86.
- 35 66. Yang, Z., et al., *Genome-wide analysis of the 5' and 3' ends of vaccinia virus early mRNAs*  
36 *delineates regulatory sequences of annotated and anomalous transcripts*. J Virol, 2011.  
37 **85**(12): p. 5897-909.
- 38 67. Yuen, L. and B. Moss, *Oligonucleotide sequence signaling transcriptional termination of*  
39 *vaccinia virus early genes*. Proc Natl Acad Sci U S A, 1987. **84**(18): p. 6417-21.
- 40 68. Unterholzner, L., et al., *Vaccinia virus protein C6 is a virulence factor that binds TBK-1*  
41 *adaptor proteins and inhibits activation of IRF3 and IRF7*. PLoS Pathog, 2011. **7**(9): p.  
42 e1002247.
- 43 69. Soday, L., et al., *Quantitative Temporal Proteomic Analysis of Vaccinia Virus Infection Reveals*  
44 *Regulation of Histone Deacetylases by an Interferon Antagonist*. Cell Rep, 2019. **27**(6): p.  
45 1920-1933 e7.
- 46 70. Parrish, S. and B. Moss, *Characterization of a vaccinia virus mutant with a deletion of the*  
47 *D10R gene encoding a putative negative regulator of gene expression*. J Virol, 2006. **80**(2): p.  
48 553-61.
- 49 71. Parrish, S. and B. Moss, *Characterization of a second vaccinia virus mRNA-decapping enzyme*  
50 *conserved in poxviruses*. J Virol, 2007. **81**(23): p. 12973-8.



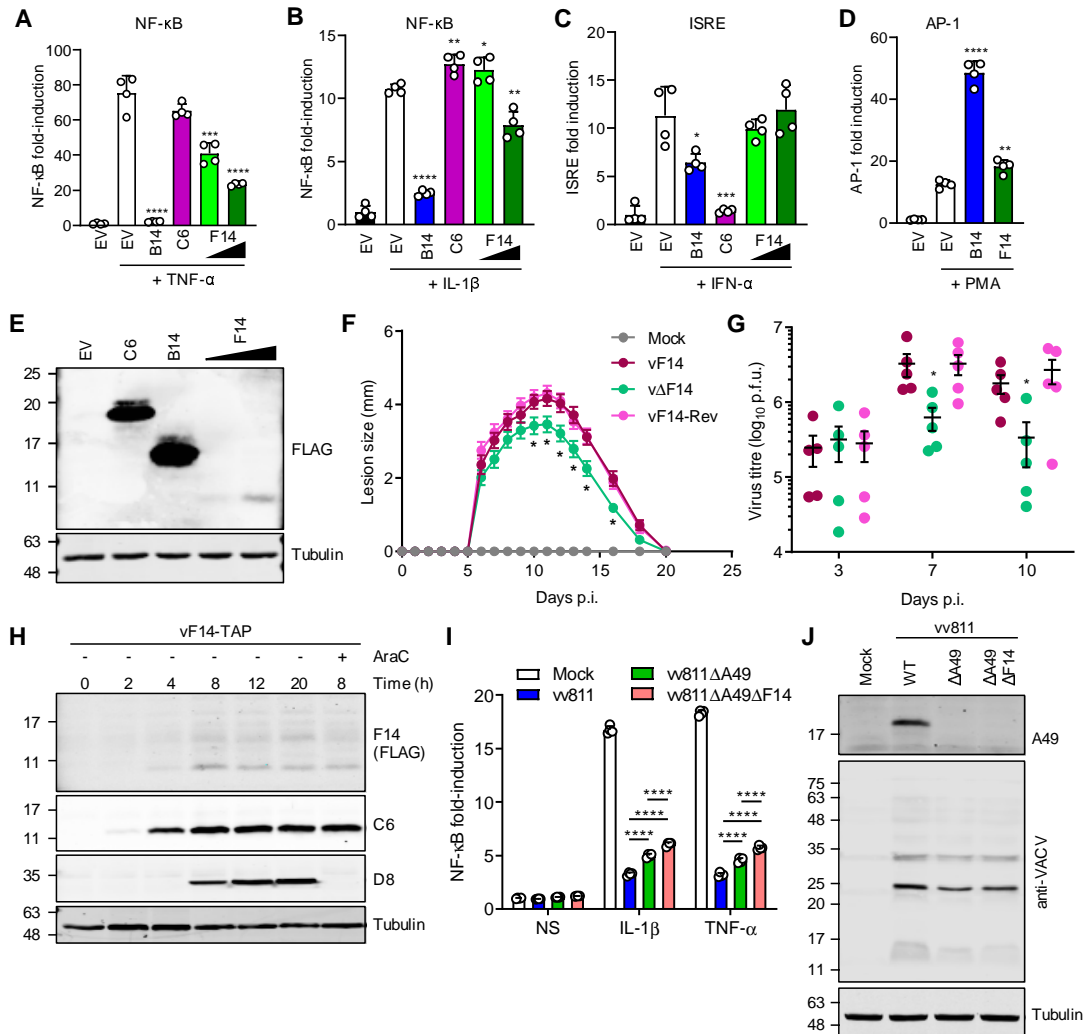
- 1 72. Ehlers, A., et al., *Poxvirus Orthologous Clusters (POCs)*. Bioinformatics, 2002. **18**(11): p. 1544-5.
- 2
- 3 73. Kelley, L.A., et al., *The Phyre2 web portal for protein modeling, prediction and analysis*. Nat Protoc, 2015. **10**(6): p. 845-58.
- 4
- 5 74. Lecoq, L., et al., *Structural characterization of interactions between transactivation domain 1 of the p65 subunit of NF-kappaB and transcription regulatory factors*. Nucleic Acids Res, 2017. **45**(9): p. 5564-5576.
- 6
- 7
- 8 75. Schmitz, M.L., et al., *Structural and functional analysis of the NF-kappa B p65 C terminus. An acidic and modular transactivation domain with the potential to adopt an alpha-helical conformation*. J Biol Chem, 1994. **269**(41): p. 25613-20.
- 9
- 10
- 11 76. Schmitz, M.L. and P.A. Baeuerle, *The p65 subunit is responsible for the strong transcription activating potential of NF-kappa B*. EMBO J, 1991. **10**(12): p. 3805-17.
- 12
- 13 77. Shi, J. and C.R. Vakoc, *The mechanisms behind the therapeutic activity of BET bromodomain inhibition*. Mol Cell, 2014. **54**(5): p. 728-36.
- 14
- 15 78. Xing, J., et al., *Herpes simplex virus 1-encoded tegument protein VP16 abrogates the production of beta interferon (IFN) by inhibiting NF-kappaB activation and blocking IFN regulatory factor 3 to recruit its coactivator CBP*. J Virol, 2013. **87**(17): p. 9788-801.
- 16
- 17
- 18 79. Huang, S.M. and D.J. McCance, *Down regulation of the interleukin-8 promoter by human papillomavirus type 16 E6 and E7 through effects on CREB binding protein/p300 and P/CAF*. J Virol, 2002. **76**(17): p. 8710-21.
- 19
- 20
- 21 80. Richards, K.H., et al., *The human papillomavirus (HPV) E7 protein antagonises an Imiquimod-induced inflammatory pathway in primary human keratinocytes*. Sci Rep, 2015. **5**: p. 12922.
- 22
- 23 81. Spitkovsky, D., et al., *The human papillomavirus oncoprotein E7 attenuates NF-kappa B activation by targeting the Ikappa B kinase complex*. J Biol Chem, 2002. **277**(28): p. 25576-82.
- 24
- 25
- 26 82. Vandermark, E.R., et al., *Human papillomavirus type 16 E6 and E 7 proteins alter NF-kB in cultured cervical epithelial cells and inhibition of NF-kB promotes cell growth and immortalization*. Virology, 2012. **425**(1): p. 53-60.
- 27
- 28
- 29 83. Pallett, M.A., et al., *Vaccinia Virus BBK E3 Ligase Adaptor A55 Targets Importin-Dependent NF-kappaB Activation and Inhibits CD8(+) T-Cell Memory*. J Virol, 2019. **93**(10).
- 30
- 31 84. Eaglesham, J.B., et al., *Viral and metazoan poxins are cGAMP-specific nucleases that restrict cGAS-STING signalling*. Nature, 2019. **566**(7743): p. 259-263.
- 32
- 33 85. Hargreaves, D.C., T. Horng, and R. Medzhitov, *Control of inducible gene expression by signal-dependent transcriptional elongation*. Cell, 2009. **138**(1): p. 129-45.
- 34
- 35 86. Mukherjee, S.P., et al., *Analysis of the RelA:CBP/p300 interaction reveals its involvement in NF-kappaB-driven transcription*. PLoS Biol, 2013. **11**(9): p. e1001647.
- 36
- 37 87. McCraith, S., et al., *Genome-wide analysis of vaccinia virus protein-protein interactions*. Proc Natl Acad Sci U S A, 2000. **97**(9): p. 4879-84.
- 38
- 39 88. Bravo Cruz, A.G. and J.L. Shisler, *Vaccinia virus K1 ankyrin repeat protein inhibits NF-kappaB activation by preventing RelA acetylation*. J Gen Virol, 2016. **97**(10): p. 2691-2702.
- 40
- 41 89. Shisler, J.L. and X.L. Jin, *The vaccinia virus K1L gene product inhibits host NF-kappaB activation by preventing IkappaBalpha degradation*. J Virol, 2004. **78**(7): p. 3553-60.
- 42
- 43 90. Diel, D.G., et al., *A nuclear inhibitor of NF-kappaB encoded by a poxvirus*. J Virol, 2011. **85**(1): p. 264-75.
- 44
- 45 91. Ning, Z., et al., *The N terminus of orf virus-encoded protein 002 inhibits acetylation of NF-kappaB p65 by preventing Ser(276) phosphorylation*. PLoS One, 2013. **8**(3): p. e58854.
- 46
- 47 92. Zou, Z., et al., *Brd4 maintains constitutively active NF-kappaB in cancer cells by binding to acetylated RelA*. Oncogene, 2014. **33**(18): p. 2395-404.
- 48
- 49 93. Sun, S.C., et al., *NF-kappa B controls expression of inhibitor I kappa B alpha: evidence for an inducible autoregulatory pathway*. Science, 1993. **259**(5103): p. 1912-5.
- 50

- 1 94. Lin, R., et al., *Virus-dependent phosphorylation of the IRF-3 transcription factor regulates*  
2 *nuclear translocation, transactivation potential, and proteasome-mediated degradation.* Mol  
3 Cell Biol, 1998. **18**(5): p. 2986-96.
- 4 95. Bhattacharya, S., et al., *Cooperation of Stat2 and p300/CBP in signalling induced by*  
5 *interferon-alpha.* Nature, 1996. **383**(6598): p. 344-7.
- 6 96. Zhang, J.J., et al., *Two contact regions between Stat1 and CBP/p300 in interferon gamma*  
7 *signaling.* Proc Natl Acad Sci U S A, 1996. **93**(26): p. 15092-6.
- 8 97. O'Connor, M.J., et al., *Characterization of an E1A-CBP interaction defines a novel*  
9 *transcriptional adapter motif (TRAM) in CBP/p300.* J Virol, 1999. **73**(5): p. 3574-81.
- 10 98. Marzio, G., et al., *HIV-1 tat transactivator recruits p300 and CREB-binding protein histone*  
11 *acetyltransferases to the viral promoter.* Proc Natl Acad Sci U S A, 1998. **95**(23): p. 13519-24.
- 12 99. Nicot, C. and R. Harrod, *Distinct p300-responsive mechanisms promote caspase-dependent*  
13 *apoptosis by human T-cell lymphotropic virus type 1 Tax protein.* Mol Cell Biol, 2000. **20**(22):  
14 p. 8580-9.
- 15 100. Patel, D., et al., *The E6 protein of human papillomavirus type 16 binds to and inhibits co-*  
16 *activation by CBP and p300.* EMBO J, 1999. **18**(18): p. 5061-72.
- 17 101. Eckner, R., et al., *Association of p300 and CBP with simian virus 40 large T antigen.* Mol Cell  
18 Biol, 1996. **16**(7): p. 3454-64.
- 19 102. Cook, J.L., et al., *Role of the E1A Rb-binding domain in repression of the NF-kappa B-*  
20 *dependent defense against tumor necrosis factor-alpha.* Proc Natl Acad Sci U S A, 2002.  
21 **99**(15): p. 9966-71.
- 22 103. Gilmore, T.D., *Multiple mutations contribute to the oncogenicity of the retroviral oncoprotein*  
23 *v-Rel.* Oncogene, 1999. **18**(49): p. 6925-37.
- 24 104. Lin, J.R., et al., *Minimalist ensemble algorithms for genome-wide protein localization*  
25 *prediction.* BMC Bioinformatics, 2012. **13**: p. 157.
- 26 105. Kall, L., A. Krogh, and E.L. Sonnhammer, *A combined transmembrane topology and signal*  
27 *peptide prediction method.* J Mol Biol, 2004. **338**(5): p. 1027-36.
- 28 106. Robert, X. and P. Gouet, *Deciphering key features in protein structures with the new*  
29 *ENDscript server.* Nucleic Acids Res, 2014. **42**(Web Server issue): p. W320-4.
- 30 107. Gloeckner, C.J., et al., *A novel tandem affinity purification strategy for the efficient isolation*  
31 *and characterisation of native protein complexes.* Proteomics, 2007. **7**(23): p. 4228-34.
- 32 108. Maluquer de Motes, C., et al., *Vaccinia virus virulence factor N1 can be ubiquitylated on*  
33 *multiple lysine residues.* J Gen Virol, 2014. **95**(Pt 9): p. 2038-2049.
- 34 109. Falkner, F.G. and B. Moss, *Transient dominant selection of recombinant vaccinia viruses.* J  
35 Virol, 1990. **64**(6): p. 3108-11.
- 36 110. Joklik, W.K., *The purification fo four strains of poxvirus.* Virology, 1962. **18**: p. 9-18.
- 37 111. Tschärke, D.C. and G.L. Smith, *A model for vaccinia virus pathogenesis and immunity based*  
38 *on intradermal injection of mouse ear pinnae.* J Gen Virol, 1999. **80** ( Pt 10): p. 2751-2755.
- 39 112. Williamson, J.D., et al., *Biological characterization of recombinant vaccinia viruses in mice*  
40 *infected by the respiratory route.* J Gen Virol, 1990. **71** ( Pt 11): p. 2761-7.

41

42

## 1 FIGURE LEGENDS



2

3 **Figure 1: Vaccinia virus protein F14 inhibits NF-κB activation and contributes to**  
 4 **virulence. (A-D)** HEK 293T cells were transfected with reporter plasmids NF-κB-Fluc (firefly  
 5 luciferase) (A, B), ISRE-Fluc (C), or AP1-Fluc (D), TK-*Renilla*, and vectors expressing the  
 6 indicated VACV proteins fused to a FLAG or tandem affinity purification (TAP) epitope or  
 7 empty vector (EV). After 16 h, cells were stimulated with TNF-α, IL-1β or IFN-α (as indicated)  
 8 for additional 8 h (A-C) or 24 h (D), when luciferase activities were measured. Means + s.d.  
 9 ( $n = 4$  per condition) are shown. (E) Aliquots from whole cell lysates prepared for dual  
 10 luciferase reporter gene assays were analysed by SDS-PAGE and immunoblotting with anti-  
 11 FLAG and anti-α-tubulin antibodies. (F) C57BL/6 mice were infected intradermally in both  
 12 ears with  $10^4$  p.f.u. of the indicated VACV strains and the lesions were measured daily with a  
 13 calliper. Means ± s.e.m. ( $n = 10$  mice) are shown. The asterisk (\*) indicates the days on  
 14 which the lesion size caused by vΔF14 was statistically different ( $P < 0.05$ ) from both vF14  
 15 and vF14-Rev. (G) Virus titres in the ears of mice infected as in (F) at 3, 7 and 10 d p.i. were  
 16 determined by plaque assay. Means ± s.e.m. ( $n = 5$  mice) are shown. (H) Immunoblot  
 17 showing F14 expression during infection. HeLa cells were infected with vF14-TAP at 5  
 18 p.f.u./cell for the indicated times and cytosine arabinoside (AraC, 40 μg/ml) was added  
 19 where indicated. Immunoblots with antibodies to FLAG (F14), VACV proteins C6 and D8,

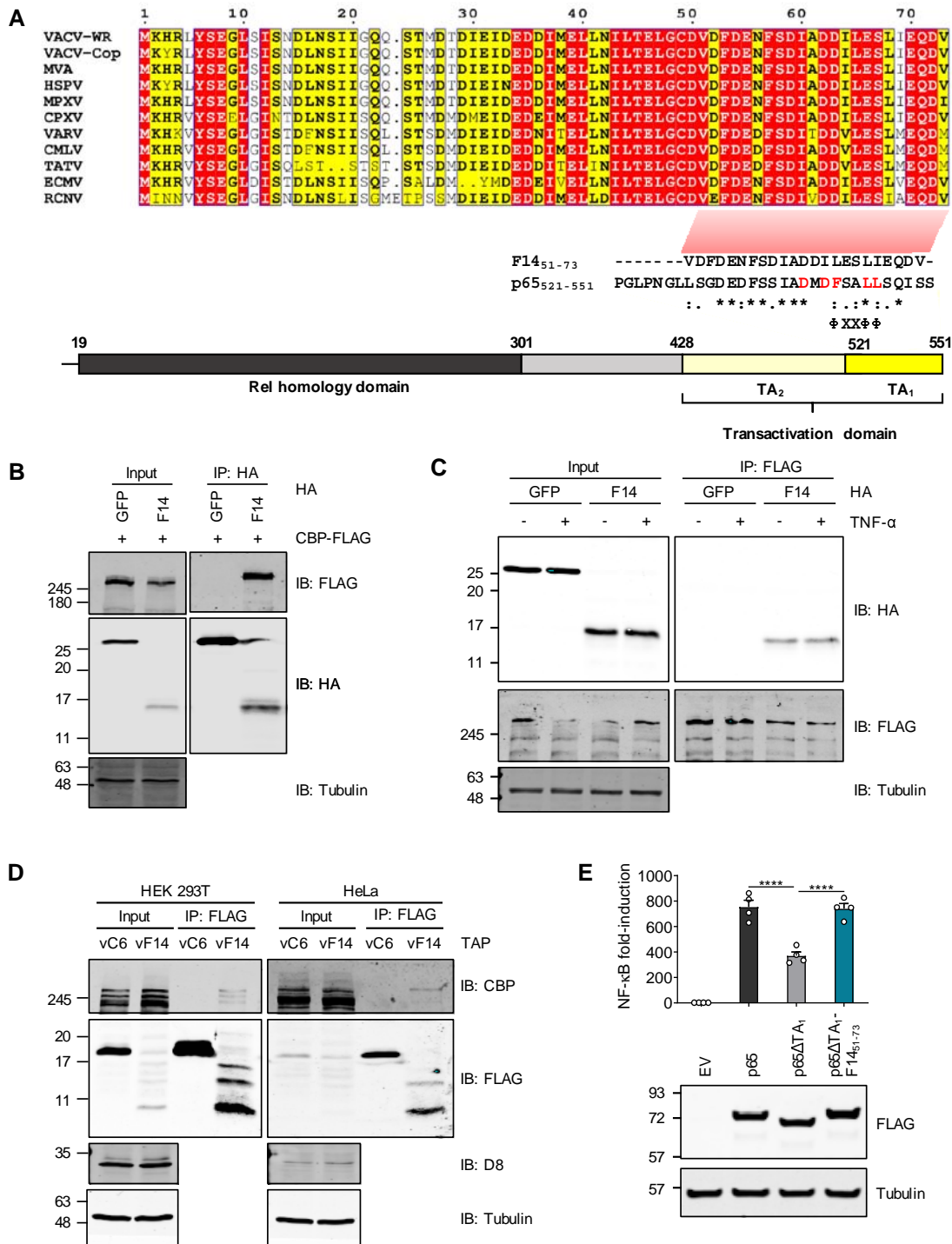
1 and  $\alpha$ -tubulin. **(I)** A549 cells transduced with reporter NF- $\kappa$ B-Fluc were infected with VACV  
2 vv811 strains at 5 p.f.u./cell. At 6 h p.i. cells were stimulated with TNF- $\alpha$  or IL-1 $\beta$  for 8 h and  
3 then luciferase activities were measured. Means + s.d. ( $n = 4$  per condition) are shown. **(J)**  
4 Immunoblots of protein extracts from A549-NF- $\kappa$ B-Fluc cells infected as indicated with  
5 antibodies against VACV protein A49, whole VACV virions, and  $\alpha$ -tubulin. **(E, H, J)** The  
6 positions of molecular mass markers in kDa are shown on the left of immunoblots. Statistical  
7 significance was determined by the Student's  $t$ -test (\*\*\*\* $P < 0.0001$ , \*\*\* $P < 0.001$ , \*\* $P < 0.01$ ,  
8 \* $P < 0.05$ ). Data shown in **(A-D, I)**, **(F, G)** and **(E, H, J)** are representative of four, two or  
9 three separate experiments, respectively.

10



1 doxycycline overnight and then stimulated with TNF- $\alpha$  for 15 min. Subcellular localisation of  
2 NF- $\kappa$ B p65 subunit was assessed by immunofluorescence. The percentages of cells  
3 displaying nuclear p65 are shown, with  $n$  (number of cells counted from two independent  
4 experiments) stated underneath each bar. (C) HEK 293T cells were transfected with reporter  
5 plasmids NF- $\kappa$ B-Fluc, TK-*Renilla*, and vectors expressing human p65-TAP, VACV proteins  
6 B14-FLAG and F14-TAP or empty vector (EV). After 24 h, luciferase activities were  
7 measured. Top panel: Means + s.d. ( $n = 4$  per condition) are shown. Statistical significance  
8 was determined by Student's  $t$ -test (\*\*\*\* $P < 0.0001$ ). Bottom panel: immunoblots of proteins  
9 detected with antibody against the FLAG epitope, and  $\alpha$ -tubulin. Protein molecular mass  
10 markers in kDa are shown on the left of the blots.

11



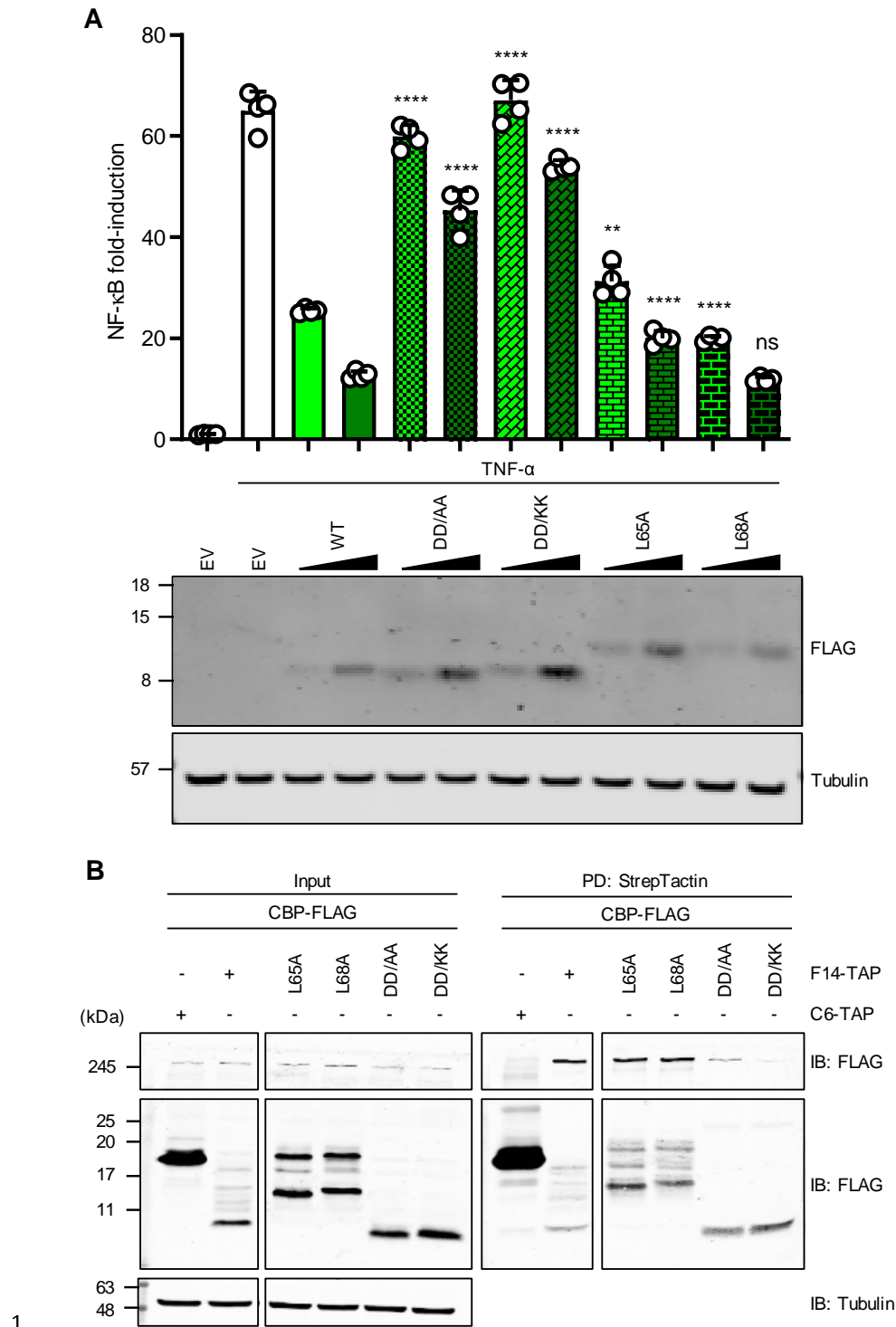
1

2 **Figure 3: F14 binds to CBP and has transactivation activity. (A)** Amino acid alignment of  
 3 F14 orthologues of representative orthopoxviruses: vaccinia virus (VACV) Western Reserve  
 4 (WR), VACV Copenhagen (Cop), modified vaccinia Ankara (MVA), horsepox virus (HSPV),  
 5 monkeypox virus (MPXV), cowpox virus (CPXV), variola virus (VARV), camelpox virus  
 6 (CMLV), taterapox virus (TATV), ectromelia virus (ECMV), and racoonpox virus (RCNV).  
 7 Red = aa identical in all sequences. Yellow = aa identical in 8/11 sequences. Alignment of  
 8 the C-termini of F14 and p65 highlighting their sequence similarity including the  $\phi$ xx $\phi$  motif,  
 9 above a schematic of p65 and its functional domains. (B, C) Lysates from HEK 293T cells

1 expressing GFP-HA, F14-HA and CBP-FLAG were immunoprecipitated with anti-HA (**B**) or  
2 anti-FLAG (**C**) and immunoblotted for FLAG- and HA-tagged proteins, and  $\alpha$ -tubulin.  
3 Immunoblots are representative of three independent experiments. (**D**) HEK 293T and HeLa  
4 cells were infected with VACV strains vC6-TAP or vF14-TAP at 5 p.f.u./cell for 8 h. Cell  
5 lysates were immunoprecipitated with anti-FLAG and immunoblotted for CBP, FLAG-tagged  
6 C6 and F14, VACV protein D8, and  $\alpha$ -tubulin. Immunoblots are representative of two  
7 independent experiments. (**E**) HEK 293T cells were transfected with NF- $\kappa$ B-Fluc, TK-*Renilla*,  
8 and vectors expressing human p65-TAP, or p65-TAP mutants or empty vector (EV). Top  
9 panel: After 24 h, luciferase activities were measured. Means + s.d. ( $n = 4$  per condition) are  
10 shown. Statistical significance was determined by the Student's *t*-test (\*\*\*\* $P < 0.0001$ ).  
11 Bottom panel: immunoblots of p65 (anti-FLAG) and  $\alpha$ -tubulin. Protein molecular mass  
12 markers in kDa are shown on the left of the blots.

13

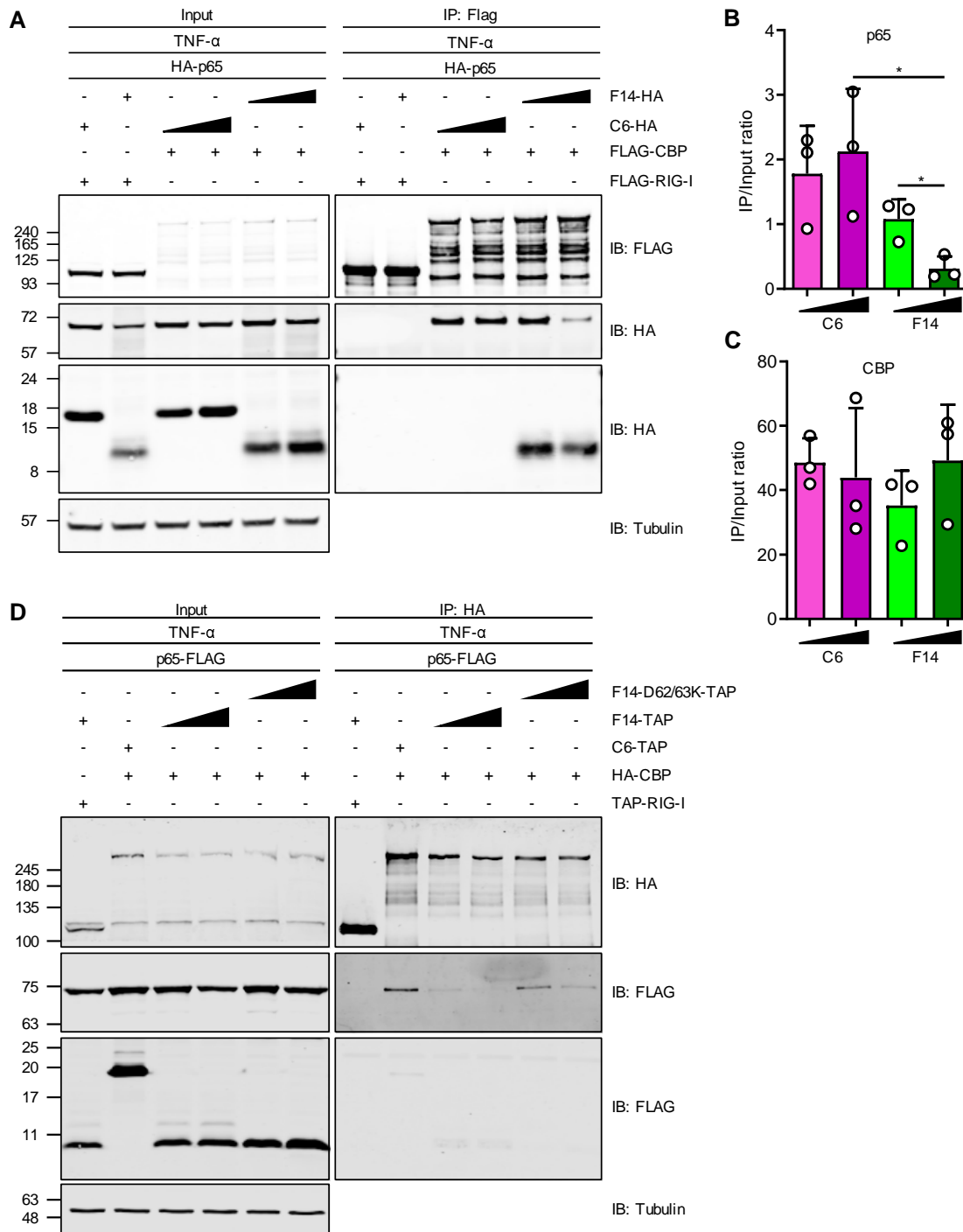




1  
2 **Figure 4: The dipeptide Asp<sup>62/63</sup> of F14 is required for inhibition of NF-κB.** (A) HEK  
3 293T cells were transfected with NF-κB-Fluc, TK-*Renilla*, and increasing concentrations of  
4 vectors expressing VACV protein F14 or the indicated mutants, or empty vector (EV). After  
5 16 h, cells were stimulated with TNF-α for 8 h, and then luciferase activities were measured.  
6 Top panel: Means + s.d. (*n* = 4 per condition) are shown. Bottom panel: Immunoblots.  
7 Aliquots of whole cell lysates prepared for dual luciferase reporter gene assays were blotted  
8 with antibodies against FLAG and α-tubulin. Data are representative of three independent

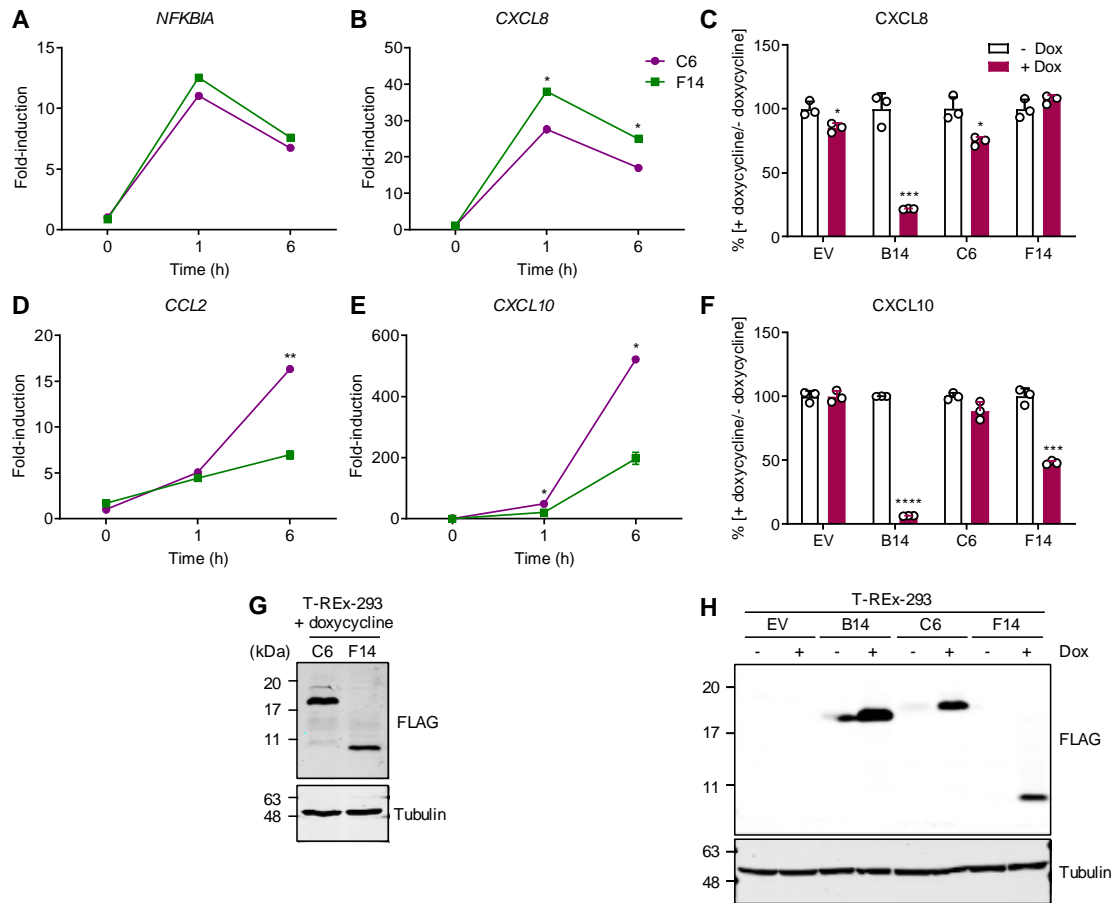
1 experiments. Statistical significance was determined by the Student's *t*-test (\*\*\*\*P < 0.0001,  
2 \*\*\*P<0.001, \*\*P < 0.01, \*P < 0.05). (B) Lysates from HEK 293T cells expressing the  
3 indicated proteins were affinity purified with StrepTactin resin and immunoblotted for FLAG  
4 and  $\alpha$ -tubulin. Immunoblots are representative of three independent experiments. DD/AA  
5 denotes D62/63A mutant and DD/KK, D62/63K mutant. Protein molecular mass markers in  
6 kDa are shown on the left of the blots.

7



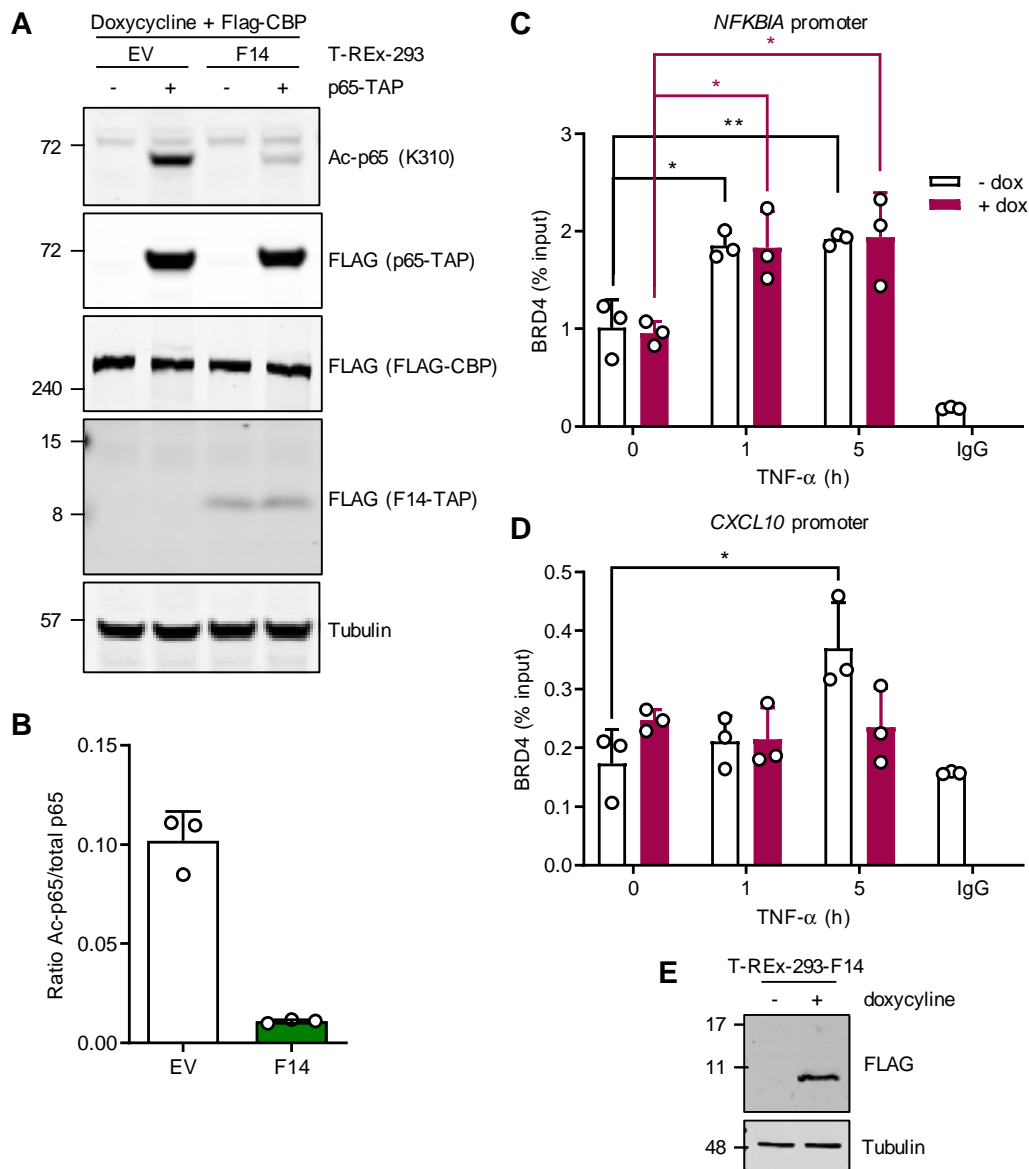
1

2 **Figure 5: F14 outcompetes NF- $\kappa$ B for binding to CBP.** (A, D) Lysates from HEK 293T  
3 cells expressing the indicated proteins and stimulated with TNF- $\alpha$  for 15 min were  
4 immunoprecipitated with anti-FLAG (A) or anti-HA (D) and immunoblotted for FLAG, HA and  
5  $\alpha$ -tubulin. Immunoblots are representative of three independent experiments. (B, C) Ratio of  
6 immunoprecipitate (IP) over input signal intensities from immunoblots as in (A). Means + s.d.  
7 ( $n = 3$  independent experiments) are shown. Statistical significance was determined by the  
8 Student's  $t$ -test (\* $P < 0.05$ ). Protein molecular mass markers in kDa are shown on the left  
9 of the blots.



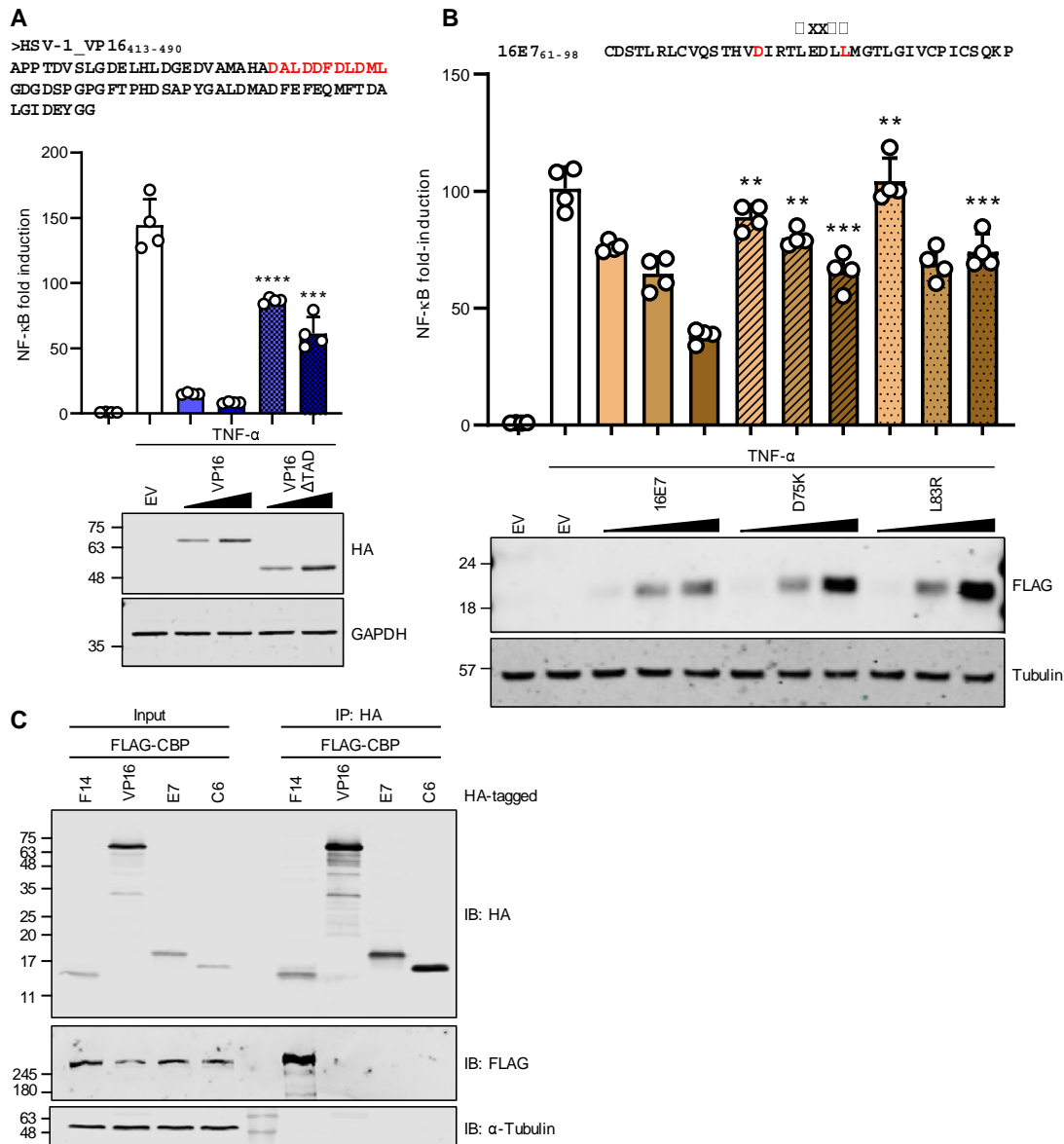
1  
2  
3  
4  
5  
6  
7  
8  
9  
10  
11  
12  
13  
14  
15

**Figure 6: F14 suppresses expression of a subset of NF-κB-responsive genes.** (A, B, D, E) T-REx-293 cells were induced with doxycycline overnight to express VACV proteins C6 or F14, and then stimulated with TNF-α for 1 or 6 h. Total RNA was extracted, and mRNA for indicated NF-κB-responsive genes was analysed by RT-qPCR. Means ± s.d. ( $n = 2$  per condition) are shown. (C, F) T-REx-293 cells inducibly expressing the empty vector (EV) or VACV proteins B14, C6 or F14 were induced with doxycycline overnight and then stimulated with TNF-α for 16 h. The concentration of CXCL8 and CXCL10 in the culture supernatants was measured by ELISA. Means + s.d. ( $n = 3$  per condition) of the percent of secretion in presence of doxycycline (+dox) in comparison to secretion in the absence of doxycycline (-dox, equals 100%) are shown. Statistical significance was determined by the Student's *t*-test (\*\*\*\* $P < 0.0001$ , \*\*\* $P < 0.001$ , \*\* $P < 0.01$ , \* $P < 0.05$ ). (G, H) Protein extracts from T-REx-293 cell lines were immunoblotted with antibodies against the FLAG or α-tubulin. Protein molecular masses in kDa are shown on the left of the blots.



1  
2  
3  
4  
5  
6  
7  
8  
9  
10  
11  
12  
13  
14  
15  
16  
17

**Figure 7: F14 antagonises p65 acetylation and BRD4 recruitment to *CXCL10* promoter.** (A) Immunoblot analysis of p65 Lys<sup>310</sup> acetylation. T-REx-293 cells stably transfected with empty vector (EV) or a plasmid inducibly expressing F14 were induced with doxycycline overnight. Cells were then transfected with plasmids for expression of p65-TAP and FLAG-CBP overnight and lysates were immunoblotted with anti-FLAG and anti- $\alpha$ -tubulin. Blots are representative of two independent experiments carried out with three biological replicates each. (B) Ratio of acetylated (Ac) p65 over total ectopic p65 signal intensities from immunoblots in (A). Means + s.d. ( $n = 3$  per condition) are shown. (C, D) T-REx-293 cells stably expressing inducible F14 were induced with doxycycline overnight before stimulation with TNF- $\alpha$  for 1 or 5 h. Chromatin immunoprecipitation (ChIP) was carried out with anti-BRD4 antibody or control IgG, and immunoprecipitated DNA was analysed by qPCR for the promoters of *NFKBIA* (C) and *CXCL10* (D) genes. Means + s.d. ( $n = 3$  per condition) are shown. Statistical significance was determined by the Student's  $t$ -test (\*\* $P < 0.01$ , \* $P < 0.05$ ). (E) Immunoblots of protein extracts from T-REx-293 cells harvested in parallel to ChIP to detect the expression of F14-FLAG and  $\alpha$ -tubulin. Protein molecular mass markers in kDa are shown on the left of the blots.



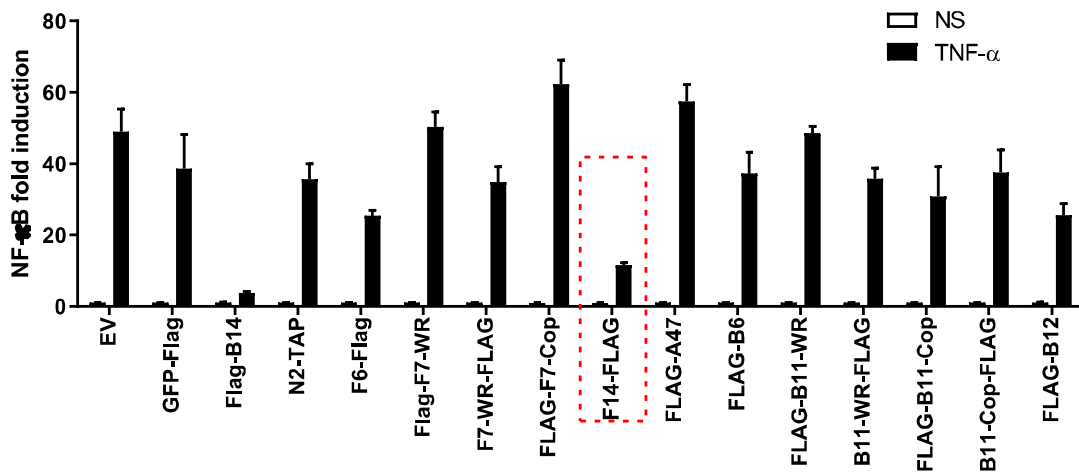
1

2 **Figure 8: F14 is a unique viral inhibitor of NF-κB.** (A) Top: Amino acid sequence of the  
 3 TAD of HSV-1 VP16 with the acidic activation domain similar to p65 highlighted in red.  
 4 Middle: HEK 293T cells were transfected with NF-κB-Fluc, TK-*Renilla* and increasing  
 5 concentrations of vectors expressing VP16 or a mutant lacking the TAD domain, or empty  
 6 vector (EV). After 16 h, cells were stimulated with TNF-α for 8 h and then luciferase activities  
 7 were measured. Means + s.d. ( $n = 4$  per condition) are shown. Bottom: Aliquots from whole  
 8 cell lysates prepared for dual luciferase reporter gene assays were immunoblotted with  
 9 antibodies against HA and GAPDH. (B) Top: Amino acid residues 61-98 from HPV16 protein  
 10 E7 encompassing a  $\phi x x \phi \phi$  motif containing and preceded by negatively charged residues.  
 11 Highlighted are two residues mutated to disrupt this motif. Middle: Wildtype 16E7 and its two  
 12 mutants (D75K and L83R) were tested in the NF-κB luciferase reporter gene assay as  
 13 described in (A). Bottom: Immunoblots with antibodies against FLAG and  $\alpha$ -tubulin.  
 14 Statistical significance was determined by the Student's *t*-test (\*\*\*\* $P < 0.0001$ , \*\*\* $P < 0.001$ ,  
 15 \*\* $P < 0.01$ ). (C) Lysates from HEK 293T cells expressing VACV F14, HSV-1 VP16, HPV E7  
 16 and VACV C6 (all HA-tagged) were immunoprecipitated with anti-HA and immunoblotted for

- 1 FLAG, HA and  $\alpha$ -tubulin. Immunoblots are representative of two independent experiments.
- 2 Protein molecular masses in kDa are shown on the left of the blots.
- 3

1 SUPPLEMENTARY MATERIAL

2

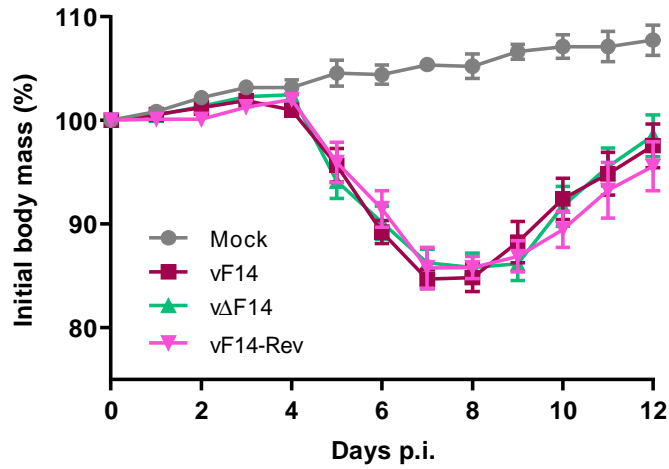


3

4 **Figure S1, related to Figure 1: Screen of VACV strain WR ORFs for NF-κB inhibitory**  
5 **activity.** HEK 293T cells were transfected with NF-κB-Fluc, TK-*Renilla*, and vectors  
6 expressing human codon-optimised and FLAG-tagged versions of the indicated VACV  
7 proteins or empty vector (EV). After 16 h, cells were stimulated with TNF-α or mock  
8 stimulated (NS) for 8 h, and then luciferase activities were measured. Means + s.d. ( $n = 4$   
9 per condition) are shown.

10





1

2 **Figure S2, related to Figure 1: Virulence of VACV mutant lacking F14 in the intranasal**  
3 **mouse model of infection.** BALB/c mice were infected intranasally with  $5 \times 10^3$  p.f.u. of the  
4 indicated VACV strains and their body mass was measured daily. Body mass is expressed  
5 as the percentage  $\pm$  s.e.m. of the mean of the same group of mice on day 0 ( $n = 10$  mice).

6

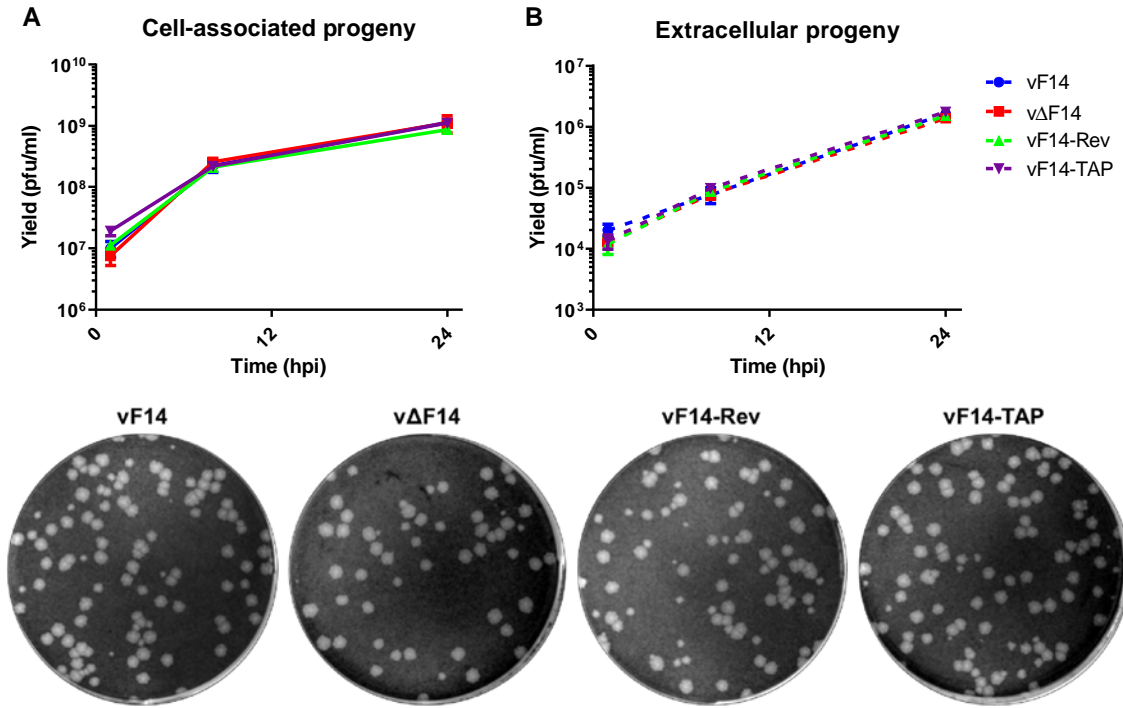
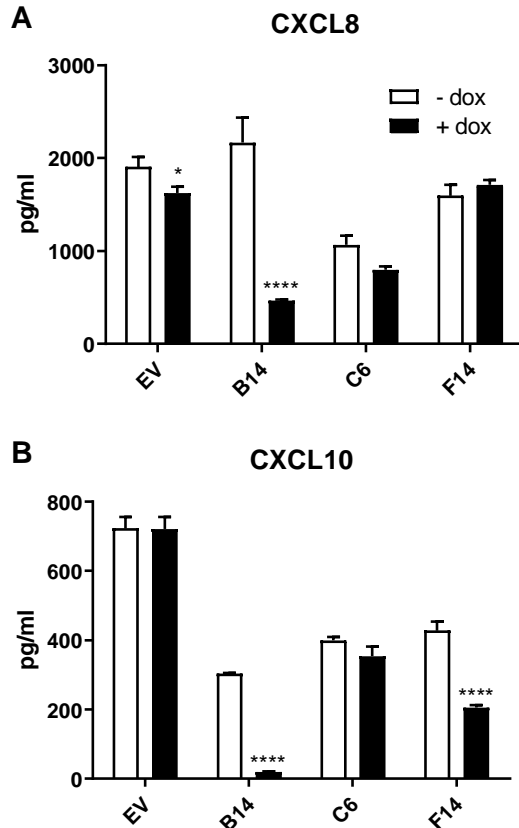


**Figure S3, related to Figure 1: Replication and spread of VACV mutant lacking F14 in cell culture.** (A, B) HeLa cells were infected with the indicated VACV strains at 5 p.f.u./cell. At 1, 12 and 24 h p.i., infectious virus titres associated with the cells (A) and in the supernatants (B) was determined by plaque assay. Means  $\pm$  s.d. (n = 4 per condition) are shown. (C) Plaque formation by the indicated VACV strains on BS-C-1 cells.



1

2 **Figure S4, related to Figure 6: F14 suppresses expression CXCL10, but not CXCL8,**  
3 **after stimulation with TNF- $\alpha$ .** This shows data normalised for presentation in **Figure 6C, F.**  
4 T-REx-293 cells stably transfected with empty vector (EV) or plasmids inducibly expressing  
5 VACV proteins B14, C6 or F14 (all TAP-tagged) were induced with doxycycline (+dox) or  
6 mock-induced (-dox) overnight and then stimulated with TNF- $\alpha$  for 16 h. The concentration  
7 of CXCL8 and CXCL10 in the supernatants from these cells was measured by ELISA.  
8 Means + s.d. ( $n = 3$  per condition) are shown. Statistical significance was determined by the  
9 Student's  $t$ -test (\*\*\*\*P < 0.0001, \*P < 0.05).

10

11 **Table S1: Oligonucleotide primers used in this study.** Primers are listed 5' to 3'.  
12 Restriction sites used are highlighted in red and indicated in parentheses following  
13 oligonucleotide sequence. If present, sequences coding the tag epitopes are highlighted in  
14 bold, whilst the Kozak sequence are shown in italics. Plasmids marked with an asterisk (\*)  
15 were constructed by site-directed mutagenesis, with the mutated codons underlined.

16

17 **Table S2: Antibodies used in this study.**